Substitutions of Glutamate 110 and 111 in the Middle Helix 4 of Human Apolipoprotein A-I (apoA-I) by Alanine Affect the Structure and in Vitro Functions of apoA-I and Induce Severe Hypertriglyceridemia in apoA-I-Deficient Mice†

Angeliki Chroni,[‡,§] Horng-Yuan Kan,[‡,§] Kyriakos E. Kypreos,[‡,§] Irina N. Gorshkova,[‡,⊥] Adelina Shkodrani,[‡] and Vassilis I. Zannis*[,‡]

Molecular Genetics, Whitaker Cardiovascular Institute, Department of Medicine, and Department of Physiology and Biophysics, Boston University School of Medicine, Boston, Massachusetts

Received January 30, 2004; Revised Manuscript Received April 23, 2004

ABSTRACT: Hypertriglyceridemia is a common pathological condition in humans of mostly unknown etiology. Here we report induction of dyslipidemia characterized by severe hypertriglyceridemia as a result of point mutations in human apolipoprotein A-I (apoA-I). Adenovirus-mediated gene transfer in apoA-I-deficient (apoA-I$^{-/-}$) mice showed that mice expressing an apoA-I[E110A/E111A] mutant had comparable hepatic mRNA levels with WT controls but greatly increased plasma triglyceride and elevated plasma cholesterol levels. In addition, they had decreased apoE and apoCII levels and increased apoB48 levels in very low-density lipoprotein (VLDL)/intermediate-density lipoprotein (IDL). Fast protein liquid chromatography (FPLC) analysis of plasma showed that most of cholesterol and approximately 15% of the mutant apoA-I were distributed in the VLDL and IDL regions and all the triglycerides in the VLDL region. Hypertriglyceridemia was corrected by coinfection of mice with recombinant adenoviruses expressing the mutant apoA-I and human lipoprotein lipase. Physicochemical studies indicated that the apoA-I mutation decreased the α-helical content, the stability, and the unfolding cooperativity of both lipid-free and lipid-bound apoA-I. In vitro functional analyses showed that reconstituted HDL (rHDL) particles containing the mutant apoA-I had 53% of scavenger receptor class B type I (SR-BI)-mediated cholesterol efflux capacity and 37% capacity to activate lecithin:cholesterol acyltransferase (LCAT) as compared to the WT control. The mutant lipid-free apoA-I had normal capacity to promote ATP-binding cassette transporter A1 (ABCA1)-dependent cholesterol efflux. The findings indicate that subtle structural alterations in apoA-I may alter the stability and functions of apoA-I and high-density lipoprotein (HDL) and may cause hypertriglyceridemia.

Apolipoprotein A-I (apoA-I)[1] is the major protein constituent of high-density lipoproteins (HDL) and plays a crucial role in the synthesis, structure, function, and plasma concentration of HDL (*1*−*5*). The biogenesis and catabolism of HDL represent a complex pathway in which participate a variety of proteins (*5*). This includes apoA-I and some minor apolipoproteins, plasma enzymes, lipid transfer proteins, and cell membrane proteins that act as lipid transporters or lipoprotein receptors. Alterations in any of these proteins may affect the levels or the functions of HDL (*5*).

It is generally believed that the initial functional interactions of lipid-free apoA-I with the ABCA1 transporter are essential for the formation of precursor HDL molecules of preβ electrophoretic mobility (*6*, *7*), which are gradually converted to discoidal and finally to spherical αHDL particles by the action of LCAT (*8*, *9*).

In vitro studies have also shown that functional interactions of discoidal rHDL and spherical αHDL with scavenger receptor class B type I (SR-BI) promote bidirectional exchange of lipids (*10*−*12*). Previous studies have associated some mutations in apoA-I (*1*, *13*−*15*) or mutations in ABCA1, which cause Tangier disease (*16*, *17*), with mild hypertriglyceridemia. However the role of apoA-I and HDL in plasma triglyceride homeostasis remains largely unknown.

Here we report association of two point mutations in the middle of helix 4 of apoA-I with dyslipidemia characterized by severe hypertriglyceridemia and elevation of plasma cholesterol levels. The E110A/E111A substitutions destabilized the lipid-free and lipid-bound apoA-I, decreased its α-helical content, and resulted in a looser tertiary structure. Previous studies using synthetic peptides had shown that residue E111 of apoA-I might be important for the activation

† This work was supported by National Institutes of Health Grants HL-33952, HL-48739, and HL-26335.

* To whom correspondence should be addressed. Tel: 617-638-5085. Fax: 617-638-5141. E-mail: vzannis@bu.edu.

‡ Department of Medicine.

§ These authors contributed equally to the work.

⊥ Department of Physiology and Biophysics.

[1] Abbreviations: ABCA1, ATP-binding cassette transporter A1; ANS, 8-anilino-1-naphthalene-sulfonate; apoA-I, apolipoprotein A-I; apoA-I$^{-/-}$ mice, apoA-I-deficient mice; BSA, bovine serum albumin; CA, carbonic anhydrase; CETP, cholesteryl ester transfer protein; DMEM, Dulbecco's modified Eagle's medium; GdnHCl, guanidine hydrochloride; DMPC, dimyristoyl-L-α-phosphatidylcholine; ELISA, enzyme-linked immunosorbent assay; FBS, fetal bovine serum; HDL, high-density lipoproteins; HEK293 cells, human embryonic kidney 293 cells; HL, hepatic lipase; LCAT, lecithin:cholesterol acyltransferase; LPL, lipoprotein lipase; NCLPDS, newborn calf lipoprotein-deficient serum; NEFA, nonesterified fatty acids; PBS, phosphate-buffered saline; POPC, β-oleoyl-γ-palmitoyl-L-α-phosphatidylcholine; rHDL, reconstituted HDL; WT, wild-type.

10.1021/bi049782p CCC: $27.50
Published on Web 07/16/2004

of LCAT (*18*). Although in the lipid-free form the mutant apoA-I had normal capacity to promote ABCA1-mediated lipid efflux, when bound to rHDL it had 37% and 53% capacity to activate LCAT and to promote SR-BI-mediated cholesterol efflux, respectively, as compared with the WT apoA-I. These data represent the first report of direct association of structural alterations in apoA-I with severe hypertriglyceridemia and indicate an important role of apoA-I and HDL in plasma triglyceride homeostasis.

EXPERIMENTAL PROCEDURES

Materials. DNA modifying enzymes were purchased from New England Biolabs, Inc. (Beverly, MA). Oligonucleotides for PCR and LipofectAMIN-2000 were purchased from Invitrogen Corp. (Carlsbad, CA). [1,2-^{3}H]Cholesterol (1 mCi/mL, specific activity range 40−60 Ci/mmol), [4-^{14}C]cholesterol (0.04 mCi/mL, specific activity 45 mCi/mmol), and materials for polymerase chain reaction (PCR) were obtained from Perkin-Elmer Life Sciences, Inc. (Boston, MA). HiTrap Q HP, HiPrep Sephacryl S-200, and Sepharose 6PC columns were from Amersham Biosciences (Piscataway, NJ). Phenyl-Sepharose CL-4B resin and bovine serum albumin (BSA) were from Sigma Aldrich Corp. (St. Louis, MO). All other reagents were purchased from Sigma Aldrich Corp. (St. Louis, MO), Bio-Rad (Hercules, CA), Fisher Scientific International, Inc. (Suwanee, GA), or other standard commercial sources described previously (*2*).

Generation and Characterization of Adenoviruses Expressing the WT and the Mutant apoA-I Forms and Production and Purification of apoA-I Using the Adenovirus System. The construction of recombinant adenoviruses carrying the genomic sequence for the WT proapoA-I has been described before (*19*). ApoA-I expressed by the adenovirus system contains the six amino acid long prosegment. The adenovirus expressing proapoA-I[E110A/E111A] was generated in a similar way. Briefly, the fourth exon of the human apoA-I gene was amplified and mutagenized by polymerase chain reaction, using a set of specific mutagenic primers, AI 110/111F and AI 110/111R, containing the mutation of interest and a set of flanking universal primers (AINOTF, AISALR) containing the restriction sites *Not*I and *Sal*I (Figure 1). The sequences of the primers are shown in Table 1. The pUCA-I_N* vector, which contains a *Not*I site in intron 3 and a *Xho*I site in the 3′-end of the apoA-I gene, was used as a template in the amplification reactions (*3*). The DNA fragment containing the mutation of interest was digested with *Not*I and *Sal*I to obtain a 1030 bp DNA fragment containing the mutated exon 4 sequence and a portion of the third intron and the 3′ flanking region. This mutated sequence was cloned into the *Not*I and *Xho*I sites of the pCA13-AIgN vector, thus replacing the WT with the mutated exon 4 sequence (Figure 1). The pCA13-AI plasmids containing the E110A/E111A mutation along with a helper PJM17 adenovirus plasmid were used to transfect 293 cells to generate recombinant adenoviruses expressing the mutant apoA-I form as described (*19*). Isolated viral plaques containing the putative recombinant adenoviruses were used to infect new cell cultures in 12-well plates of 293 cells, and 72 h postinfection, the media were analyzed by SDS−PAGE and immunoblotting using human apoA-I antibodies (Ottawa Heart Institute Research Company). Positive recombinant adenoviruses were subjected to three rounds of plaque purification using 911 cells.

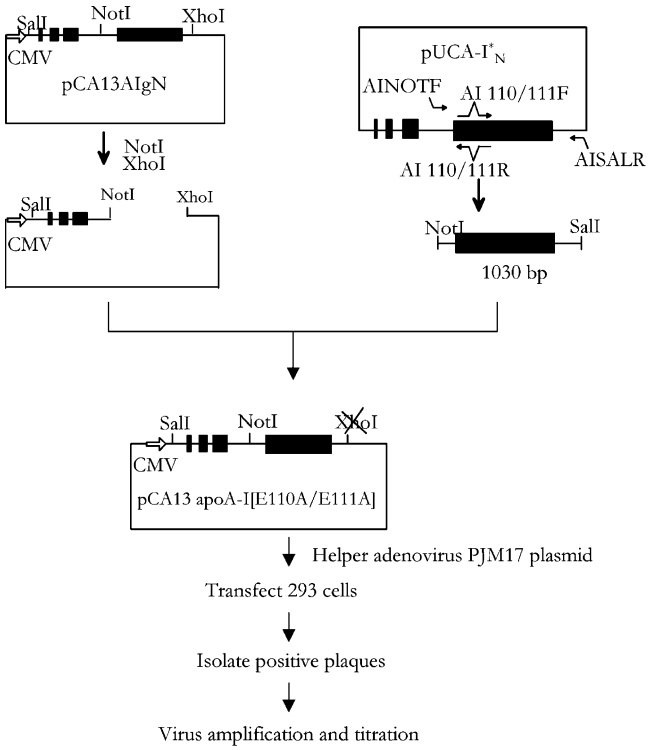

FIGURE 1: Cloning steps leading to the generation of recombinant adenovirus expressing apoA-I[E110A/E111A]. The coding sequence of the gene for wild-type apoA-I was inserted into the adenovirus shuttle vector pCA13 to generate the pCA13-AIgN plasmid (19). A fragment of genomic DNA containing the mutations, which extends from the third intron to the 3′-flanking region, was generated by PCR amplification and mutagenesis of an apoA-I-containing plasmid (pUCA-I_N*). This fragment, following digestion with *Not*I and *Sal*I, was used to replace the wild-type *Not*I/*Xho*I gene fragment in the pCA13-AIgN plasmid. The pCA13 apoA-I[E110A/E111A] plasmid containing the apoA-I mutant, along with a helper PJM17 adenovirus plasmid, were used to transfect 293 cells and generate recombinant adenoviruses expressing the mutant apoA-I form.

Following large scale infection of 293 cell cultures with the recombinant adenoviruses, the adenoviruses were purified by two consecutive $CsCl_2$ density gradient ultracentrifugation steps, dialyzed and titrated (*19*). The titers of the viruses were generally between 1×10^{10} and 5×10^{10} pfu/mL.

For apoA-I production, human HTB13 cells (SW 1783, human astrocytoma) grown to 80% confluence in Leibovitz's L-15 medium containing 10% (v/v) fetal bovine serum (FBS) in roller bottles were infected with adenoviruses expressing WT proapoA-I and proapoA-I[E110A/E111A] at a multiplicity of infection of 20. After 24 h of infection, cells were washed twice with serum-free medium and preincubated in serum-free medium for 30 min, and fresh serum-free medium was added. After 24 h, the medium was harvested, and fresh serum-free medium was added to the cells. The harvests were repeated approximately 8−10 times.

The proteins were purified from the serum-free medium by ion exchange chromatography followed by gel filtration, as described previously (*2*, *3*). For assessing secretion of WT apoA-I and the apoA-I[E110A/E111A] mutant, HTB-13 cultures in 100 mm diameter dishes were infected as above. Twenty-four hours postinfection, cells were washed twice with phosphate-buffered saline (PBS) and preincubated in serum-free medium for 2 h. Following an additional wash with PBS, fresh serum-free medium was added. After 24 h

Table 1: Oligonucleotide Sequence of Primers Used in PCR Amplifications[a]

name	sequence	location of sequence
AI 110/111F	5′-TTCCAGAAGAAGTGGCAGG**C**GG**C**GATGGAGCTCTACCGCCAG-3′	nt 1422−1463 of pUCA-I_N* vector (sense; amino acids +104 to +132)
AI 110/111R	5′-CTGGCGGTAGAGCTCCATC**G**CC**G**CCTGCCACTTCTTCTGGAA-3′	nt 1463−1422 of pUCA-I_N* vector (antisense; amino acids +132 to +104)
AINOTF	5′-CCTCCGCGGACAGGCGGCCGCCAGGG-3′	nt 1153−1178 of pUCA-I_N* vector, intron 3 of apoA-I gene
AISALR	5′-ACATGTTCGACCCCCTTTCAGGGCACCTGGCCTG-3′	ACAT + *Sal*I site of pUCA-I_N* vector at the 3′ end of apoA-I gene

[a] Boldface letters indicate nucleotide substitutions.

of incubation, medium was collected and analyzed by enzyme-linked immunoabsorbent assay (ELISA) and SDS−PAGE.

Adenoviruses Expressing Human Lipoprotein Lipase (LPL) and Human LCAT. The adenoviruses expressing WT and an inactive form of human lipoprotein lipase having an S132T substitution, as well as human LCAT, were a generous gift of Dr. Santamarina-Fojo (*20*−*22*).

Animal Studies. Male apoA-I-deficient mice (apoA-$I^{-/-}$), ($ApoA1^{tm1Unc}$) C57BL/6J mice (*23*), were purchased from Jackson Laboratories (Bar Harbor, ME). The mice were maintained on a 12-h light/dark cycle and standard rodent chow. The mice were 6−8 weeks old at the time of injection of the adenoviruses. All procedures performed on the mice were in accordance with National Institutes of Health and institutional guidelines. The apoA-$I^{-/-}$ mice were injected via the tail vein with 3×10^8 to 2×10^9 pfu of recombinant adenovirus per animal, and the animals were sacrificed 4 days postinjection following a 4-hour fast. The plasma of the mice was adjusted to 1 mM phenyl methyl sulfonyl fluoride, 0.2% (w/v) aprotinin, 0.1% (w/v) EDTA, and 0.002% (w/v) sodium azide prior to analysis of lipids, lipoproteins, and apoA-I.

Plasma Lipids and apoA-I Levels, FPLC Profiles, and Steady-State Hepatic Human apoA-I mRNA Levels. The concentration of cholesterol and triglycerides in plasma was determined using the INFINITY cholesterol reagent and INFINITY triglyceride reagent (Sigma Aldrich Corp.) according to the manufacturer's instructions. Cholesterol and triglycerides concentrations were determined spectrophotometrically at 490 nm. The concentration of human apoA-I in plasma was determined by sandwich ELISA (*4*). Mouse monoclonal anti-human apoA-I antibodies 5F6 (University of Ottawa Heart Institute; the epitope is amino acids 118−141 of the human apoA-I) were used for coating a microtiter plate and sheep polyclonal anti-human apoA-I coupled to horseradish peroxidase (Biodesign International) was used as a secondary antibody. The immunoperoxidase procedure was employed for the colorimetric detection of apoA-I at 490 nm using *o*-phenylenediamine dihydrochloride as substrate.

For FPLC analysis of plasma samples, 8−16 μL of plasma of mice infected with adenovirus-expressing WT apoA-I or apoA-I[E110A/E111A] were loaded onto a Sepharose 6 PC column in a SMART micro FPLC system (Amersham Biosciences) and eluted with PBS. A total of 25 fractions of 50 μL volume each were collected for further analysis. The concentration of cholesterol, triglycerides, and apoA-I in the FPLC fractions was determined as described above.

Total cellular RNA was isolated from the mouse liver using the Trizol procedure (Invitrogen Corp.) as recommended by the manufacturer. Fifteen micrograms of total RNA was separated on 1.0% agarose−formaldehyde gels, transferred to Hybond-N+ nylon membrane (Amersham Biosciences), and cross-linked to the membrane by UV irradiation (Stratalinker, Stratagene). The apoA-I probe used for hybridization contained 290 bp of exon 4 of human apoA-I and 148 bp of the intergenic sequence between the apoA-I and apoCIII genes. The mouse GAPDH probe (905 bp) was obtained from Ambion. The probes were labeled with ^{32}P using the Multiprime DNA labeling system (Amersham Biosciences). Quantitation of the bands on the X-ray film was performed by a phosphorimager (Molecular Dynamics) using the ImageQuant program. The apoA-I mRNA signal was normalized for the GAPDH mRNA signal (*24*).

Fractionation of Plasma by Density Gradient Centrifugation and Electron Microscopy Analysis of the apoA-I-Containing Fractions. For this analysis, 300 μL of plasma obtained from adenovirus-infected mice was diluted with saline to a total volume of 2 mL. The mixture was adjusted to density 1.23 g/mL with KBr and overlayed with 1 mL each of KBr solutions of $d = 1.20$ and $d = 1.15$ g/mL followed by 3 mL each of KBr solutions of $d = 1.06$ and $d = 1.019$ g/mL, followed by 3 mL of saline solution. The mixture was centrifuged for 20 h in an SW41 rotor at 32,000 rpm. Following ultracentrifugation, 1 mL fractions were collected from the top for further analyses. The refractive index of the fractions was measured using a refractometer (American Optical Corp.), and it was converted to density for each sample on the basis of a standard curve derived from solutions of known densities. The fractions were dialyzed against ammonium acetate and carbonate buffer (126 mM ammonium acetate, 2.6 mM ammonium carbonate, 0.26 mM EDTA, pH 7.4). Aliquots of the fractions were analyzed by SDS−PAGE and Western blotting. The nitrocellulose membranes were probed with the goat polyclonal anti-human apoA-I antibody (Chemicon International). The apoA-I bands were visualized by chemiluminescence following incubation with rabbit anti-goat IgG (Biodesign International) coupled to horseradish peroxidase. This analysis showed the distribution of apoA-I in different density regions. Fractions containing the highest concentrations of apoA-I were analyzed by electron microscopy.

To isolate proteins floating in the very low-density lipoprotein (VLDL)/intermediate-density lipoprotein (IDL) region, a different fractionation protocol was used. An aliquot of 0.3 mL of plasma obtained from adenovirus-infected mice was diluted with saline to a total volume of 0.5 mL. The

mixture was adjusted to a density of 1.23 g/mL with KBr and overlayed with 1 mL of KBr solution of $d = 1.21$ g/mL, 2.5 mL of KBr solution of $d = 1.063$ g/mL, 0.5 mL of KBr solution of $d = 1.019$ g/mL, and 0.5 mL of normal saline. The mixture was centrifuged for 22 h in an SW55 rotor at 30,000 rpm. Following ultracentrifugation, 0.5 mL fractions were collected from the top and dialyzed as described above. The first fraction was analyzed by SDS−PAGE and Western blotting. The nitrocellulose membranes were probed with goat polyclonal anti-mouse apoB, apoE, and apoCII antibodies (Santa Cruz Biotechnology, Inc. Santa Cruz, CA).

For electron microscopy analysis, the fractions that float in the HDL region were dialyzed against ammonium acetate and carbonate buffer. The samples were applied on carbon-coated grids, stained with sodium phosphotungstate, visualized in the Phillips CM-120 electron microscope (Phillips Electron Optics, Eindhoven, Netherlands), and photographed as described previously (*25*). The photomicrographs were taken at 75,000× magnification and enlarged 3 times.

Preparation and Electron Microscopy Analysis of rHDL Containing POPC/Cholesterol/apoA-I. rHDL particles were prepared by the sodium cholate dialysis method (*26*) using POPC/cholesterol/apoA-I/sodium cholate in a molar ratio of 100:10:1:100, as previously described (*3*). The rHDL samples were adjusted either by dilution or by concentration to a final protein concentration of approximately 1 mg/mL and photographed as described above.

Rate of VLDL Triglyceride Production in apoA-I$^{-/-}$ Mice Infected with WT apoA-I and the apoA-I[E110A/E111A] Mutant. VLDL triglyceride secretion was determined as described (*27*).

In Vitro Lipolysis of Triglycerides of the VLDL Plasma Fraction. Increasing concentrations of the VLDL/IDL fraction obtained from plasma of apoA-I-deficient mice expressing WT apoA-I and apoA-I[E110A/E111A] mutant were used as substrate in lipolysis experiments. Aliquots of VLDL/IDL in a final volume of 40 μL were adjusted to 2% fatty acid-free BSA, 100 mM Tris-HCl, pH 8.5, and were incubated with 34 ng of LPL (Sigma, St. Louis, MO) for 15 min at 37 °C. The released free fatty acids were quantified using an enzymatic colorimetric reagent, NEFA C (Wako Chemicals, Germany). Background values were determined by omitting LPL for each substrate concentration. LPL activity is expressed as micromoles of nonesterified fatty acid released per hour per millgram of LPL. Apparent K_m and apparent V_{max} values of the enzymatic reaction were calculated using the Prism software (GraphPad Software, Inc.).

Effect of WT apoA-I and apoA-I[E110A/E111A] Mutant on the Activity of Lipoprotein Lipase. LPL activity was assayed as previously described with modification (*28*, *29*). Liposyn III, 10% containing 100 mM triglycerides and 15.8 mM phospholipids in emulsion (Abbott Laboratories, Chicago, IL), was used as a substrate. The lipid emulsion substrate at 0.7 mM of triglycerides was preincubated at 37 °C for 20 min with 2% fatty acid-free BSA, 100 mM Tris-HCl, pH 8.5, 10% fasting plasma obtained from apoA-I-deficient mice, and various concentrations of purified WT or mutant forms of apoA-I at a total volume of 40 μL. Fasting plasma of apoA-I-deficient mice that was used as a source of LPL activator apoCII was heat-inactivated at 56 °C for 1 h prior to use to inactivate any endogenous LPL. Triglyceride lipolysis was initiated by addition of 34 ng of LPL (Sigma, St. Louis, MO), and the reaction mixture was incubated for 15 min at 37 °C. The released free fatty acids during the lipolysis were measured using an enzymatic colorimetric reagent, NEFA C (Wako Chemicals, Germany), according to the manufacturer's directions. Samples without the addition of LPL were assayed in parallel, and the background values were subtracted.

ABCA1 Expression Plasmid. The expression plasmid of human ABCA1 was a generous gift of Dr. M. W. Freeman and was constructed as described (*30*).

ABCA1 and SR-BI-Mediated Efflux of [^{3}H]Cholesterol. For determination of ABCA1-mediated cholesterol efflux, 95% confluent HEK293 EBNA-T cell cultures grown in high-glucose DMEM in 24-well plates were transfected using LipofectAMIN-2000 with either a pcDNA ABCA1 expression plasmid or the empty pcDNA vector. Sixteen hours following transfection, cells were labeled with [1,2-^{3}H]-cholesterol for 24 h and incubated with 1 μM WT or mutant apoA-I form for 4 h as described (*2*, *30*). The media were collected and clarified by centrifugation in a microcentrifuge for 2 min, and the radioactivity in 300 μL of the supernatant was determined by liquid scintillation counting. The cells were lysed with 1 mL of 0.1 M NaOH, and the radioactivity in a 300 μL aliquot of the cell lysate was determined by scintillation counting. [^{3}H]Cholesterol efflux was expressed as the percentage of the radioactivity released in the medium relative to the total radioactivity in cells and medium. To calculate the net ABCA1-mediated efflux, the cholesterol efflux of the cells transfected with the control plasmid (mock) was subtracted from the cholesterol efflux of the cells transfected with the ABCA1 plasmid.

For determination of SR-BI-mediated efflux of [^{3}H]-cholesterol, the ldlA[mSR-BI] cell line, which expresses the mouse SR-BI, or the parent ldlA-7 cell line were used (*31*, *32*). LdlA[mSR-BI] and ldlA-7 cells were plated in 6-well plates in Ham's F-12 medium at 2×10^5 cells/well and were labeled on day 1 with [1,2-^{3}H]cholesterol and treated as described (*4*). On day 4, cells were incubated with 1 μM rHDL containing the WT and the mutant apoA-I form. At various time points, 65 μL of culture medium were removed from the wells and clarified by centrifugation for 1 min in a microcentrifuge. The radioactivity in 50 μL of the supernatant was then measured by liquid scintillation counting. At the end of the incubation, the remaining culture medium was discarded, and the cells were lysed in 800 μL of lysis buffer (PBS and 1% Triton X-100) for 30 min at room temperature. The radioactivity in 100 μL of each cell lysate was determined by liquid scintillation counting, and the percent of efflux was calculated. Total cellular [^{3}H]cholesterol was calculated as the sum of the radioactivity in the efflux medium plus the radioactivity in the cell lysate. The percent of [^{3}H]cholesterol efflux represents cholesterol released into the culture medium at different times, divided by the total cholesterol, and multiplied by 100. To calculate the net SR-BI-mediated efflux, the cholesterol efflux of the untransfected ldlA-7 cells was subtracted from the cholesterol efflux of the SR-BI-expressing cells.

LCAT Production, Purification and Activation by WT and Mutant apoA-I Forms. LCAT was purified from the culture medium of human HTB13 cells infected with an adenovirus expressing the human LCAT cDNA (*21*). The cells were grown in roller bottles as described above in serum-free

Leibovitz's L-15 medium without phenol red, the medium was collected, and LCAT was purified by chromatography on a Phenyl-Sepharose CL-4B column as described (*33*, *34*). Briefly, 450 mL of medium were adjusted to 0.3 M NaCl and passed through a 50 mL Phenyl-Sepharose CL-4B column at a rate of 1.5 mL/min. The column had been equilibrated with 5 mM sodium phosphate, pH 7.4, 0.3 M NaCl. The column was washed with the same buffer until absorbance at 280 nm was below 0.01. Subsequently, LCAT was eluted with deionized H_2O (four column volumes) at the same flow rate. The fractions were adjusted to 5 mM sodium phosphate, pH 7.4, 5 mM EDTA and analyzed by Western blot using mouse anti-human LCAT antibodies 5D4 (University of Ottawa Heart Institute), and those containing the LCAT protein were pooled and further concentrated using a Centriplus concentrator (Amicon) with a molecular weight cutoff of 10,000. The final enzyme preparation adjusted to 10% glycerol was divided to aliquots and stored at −80 °C. For LCAT analysis, the substrate cholesterol and [^{14}C]-cholesterol−POPC−apoA-I rHDL particles were prepared as described above by the sodium cholate dialysis method (*26*) using POPC/cholesterol and [^{14}C]cholesterol (5000−7000 cpm of [^{14}C]cholesterol per nanomole of unlabeled cholesterol)/apoA-I/sodium cholate at a molar ratio of 100:10:1:100 (3). The rHDL were diluted in buffer (10 mM Tris-HCl, pH 8, 150 mM NaCl, and 0.01% EDTA) to give apoA-I concentrations ranging from 5×10^{-8} to 2.5×10^{-6} M in a final 0.5 mL reaction mixture. Each reaction mixture contained 50 μL of 50 mg/mL BSA, 20 μL of 100 mM β-mercaptoethanol, and sufficient quantity of the LCAT solution necessary to keep the extent of cholesterol esterification below 15%. The reaction was carried out for 30 min at 37 °C, and the conversion of [^{14}C]cholesterol to [^{14}C]-cholesteryl ester was determined by lipid extraction of the incubation mixture followed by thin-layer chromatography. The samples were prepared in duplicate, and background values were determined by omitting LCAT at each substrate concentration. The cholesterol esterification rate was expressed as nanomoles of cholesteryl ester formed per hour. The apparent V_{max} and K_m were determined from plots of the rate of cholesteryl ester formation as a function of the apoA-I concentration, and the data were fitted to Michaelis−Menten kinetics.

Circular Dichroism (CD) Spectroscopy. CD measurements were performed on an AVIV 62 DS spectropolarimeter (AVIV Associates, Inc.) equipped with a thermoelectric temperature control and calibrated with d_{10}-camphorsulfonic acid in 5, 2, or 1 mm path length quartz cuvettes at protein concentration 20−160 μg/mL. Far-UV CD spectra were recorded as described previously (*35*, *36*). The spectra were normalized to molar residue ellipticity using a mean residue weight of 115.3 for WT apoA-I and 114.8 for apoA-I[E110A/E111A]. The complete superimposition of the normalized spectra obtained at various protein concentrations for each recombinant apoA-I is consistent with the absence of protein self-association within the range of protein concentrations used in our experiments. The α-helix content was estimated from the molar residue ellipticity at 222 nm [Θ_{222}] (*37*). The protein concentration was determined by modified Lowry protein assay; the protein assay for rHDL was performed in the presence of SDS.

Thermal and Chemical Unfolding Monitored by CD. Thermal and chemical unfolding of lipid-free apoA-I was monitored by ellipticity at 222 nm using protein concentrations 25−80 μg/mL as described previously (*35*, *36*). For thermal unfolding, samples were heated from 0 to 98 °C with temperature step size 0.5−1 °C. For chemical unfolding, samples were incubated with different concentrations of guanidine HCl (GdnHCl). Similarly, the chemical unfolding of apoA-I in rHDL particles was monitored by ellipticity at 222 nm, following the incubation of aliquots of the particles at protein concentrations 25−160 μg/mL with various concentrations of GdnHCl (from 0 to 5 M) at 4 °C for 72 h. The midpoint (melting) temperature, T_m, and van't Hoff enthalpy, ΔH_v, of the temperature-induced transitions were determined from van't Hoff plots (*38*), ln K_{eq} versus $1/T$, where K_{eq} is the apparent equilibrium constant and T is temperature in Kelvin. The equilibrium constant was calculated as $K_{eq}(T) = (\Theta_F - \Theta_{obs})/(\Theta_{obs} - \Theta_U)$, where Θ_{obs} is the observed ellipticity and Θ_F and Θ_U are baselines for the protein folding and unfolding states determined by linear extrapolations of the pre- and posttransitional regions. In the transition region, the plots were fitted by the linear function, $\ln K_{eq} = \Delta \boldsymbol{S}/R - (\Delta H_v/R)(1/T)$, where $R = 1.98$ cal mol^{-1} K^{-1} is the universal gas constant and $\Delta \boldsymbol{S}$ is the transition entropy.

For chemical unfolding, the free energy of denaturation (conformational stability), ΔG_D°, the midpoint of denaturation, $D_{1/2}$, and m value, which reflects the steepness of the denaturation curve in the transition region, were determined using a linear extrapolation method (*39*). A plot of Gibbs free energy, $\Delta G_D = -RT \ln K_{eq}$, where $T = 25$ °C $= 298.15$ K, versus denaturant concentration, [D], was fitted by the linear function $\Delta G_D = \Delta G_D^\circ - m[D]$. The apparent equilibrium constant, K_{eq}, was calculated as shown above, except $\Theta_{obs}([D])$ is the observed ellipticity at a given concentration of GdnHCl, [D], and Θ_F and Θ_U are the ellipticities in the folded and unfolded states, respectively. Θ_F and Θ_U were taken as constants.

8-Anilino-1-naphthalene-sulfonate (ANS) Fluorescence. Fluorescence measurements were performed at 25 °C using a FluoroMax-2 fluorescence spectrometer (Instruments S.A., Inc.). ANS fluorescence emission spectra were recorded in the presence of WT apoA-I or apoA-I[E110A/E111A]; concentration of each protein was 0.05 mg/mL. ANS at a concentration of 0.25 mM in 10 mM sodium phosphate buffer (pH 8) was excited at wavelength of 395 nm with 5 nm slit width. The emission spectra were scanned from 400 to 560 nm using 2.5 nm slit width. For comparison, ANS fluorescence was recorded in the buffer in the absence of any protein and in the presence of 0.05 mg/mL carbonic anhydrase (CA) as a typical globular water-soluble protein or 0.05 mg/mL bovine serum albumin as a protein known to have hydrophobic binding pockets.

DMPC Clearance Kinetic Analysis. The initial rate of binding of WT and mutant protein to DMPC multilamellar liposomes was determined using a kinetic−turbidimetric method as described (*40*).

RESULTS

Plasma Lipids and apoA-I Levels Following Adenovirus Infection. Analysis of plasma lipids and apoA-I levels 4 days

Table 2: Comparison of Plasma Cholesterol, Triglycerides, and ApoA-I Levels and Hepatic mRNA Levels of ApoA-I$^{-/-}$ Mice Prior to Infection or 4 Days Postinfection with Recombinant Adenoviruses Expressing the WT ApoA-I or the ApoA-I[E110A/E111A] Mutant[a]

	cholesterol (mg/dL)	triglycerides (mg/dL)	apoA-I (mg/dL)	relative apoA-I mRNA (%)
WT apoA-I	272 ± 56	218 ± 85	338 ± 21	100
apoA-I[E110A/E111A]	520 ± 45	1510 ± 590	204 ± 27	69 ± 23
apoA-I$^{-/-}$	39 ± 6	47 ± 7		

[a] Plasma was obtained from apoA-I$^{-/-}$ mice prior to infection or 4 days postinfection with 1×10^9 plaque-forming units (pfu) of adenoviruses expressing WT apoA-I or the apoA-I[E110A/E111A] mutant and analyzed for cholesterol and triglyceride levels, apoA-I levels, and hepatic apoA-I mRNA levels as described in Experimental Procedures. The mRNA levels are expressed relative to that in mice infected with recombinant adenovirus expressing WT apoA-I. Values are means ± SD ($n = 3-7$).

postinfection showed that in mice infected with adenoviruses expressing the WT apoA-I and the apoA-I[E110A/E111A] mutant, the plasma apoA-I levels were high (338 and 204 mg/dL, respectively). The cholesterol and triglyceride levels, however, did not correlate with the plasma apoA-I levels. Compared with the mice expressing the WT apoA-I, mice expressing the apoA-I[E110A/E111A] mutant had significantly higher plasma cholesterol levels and displayed severe hypertriglyceridemia (Table 2).

Determination of the Levels of apoA-I Expression in Mice and Control Experiments in Cells. To assess the expression of apoA-I in apoA-I$^{-/-}$ mice infected with different doses of either the WT apoA-I or the apoA-I[E110A/E111A] mutant, total RNA was isolated from the mouse livers 4 days postinfection and analyzed for apoA-I and GAPDH mRNA levels by Northern blotting (*24*). This analysis showed that although the hepatic apoA-I mRNA levels of individual mice infected with adenoviruses expressing the WT or the mutant apoA-I forms were comparable, only the mice infected with the apoA-I[E110A/E111A] mutant developed severe hypertriglyceridemia (Figure 2; Table 2). The mice expressing the apoA-I[E110A/E111A] also had elevated cholesterol levels as compared with mice expressing the WT apoA-I. Analysis of the medium of HTB13 cells infected with adenoviruses expressing the WT apoA-I or the apoA-I[E110A/E111A] mutant by SDS−PAGE and sandwich ELISA showed that both apoA-I forms are secreted efficiently at comparable levels in the range of 60−100 μg of apoA-I per milliliter per 24 h period (Figure 3).

FPLC Profiles of Plasma Isolated from Mice Infected with Adenoviruses Expressing the WT apoA-I and the Mutant apoA-I[E110A/E111A] Form. FPLC analysis of plasma from apoA-I$^{-/-}$ mice infected with recombinant adenoviruses expressing either the WT or the mutant apoA-I form 4 days postinfection showed that in mice expressing the WT apoA-I, cholesterol was distributed predominantly in the HDL2 and HDL3 regions, whereas in mice expressing the apoA-I[E110A/E111A] mutant, cholesterol was distributed mainly in the VLDL and to a lesser extent in the HDL3 and LDL regions (Figure 4A). The triglycerides in mice expressing

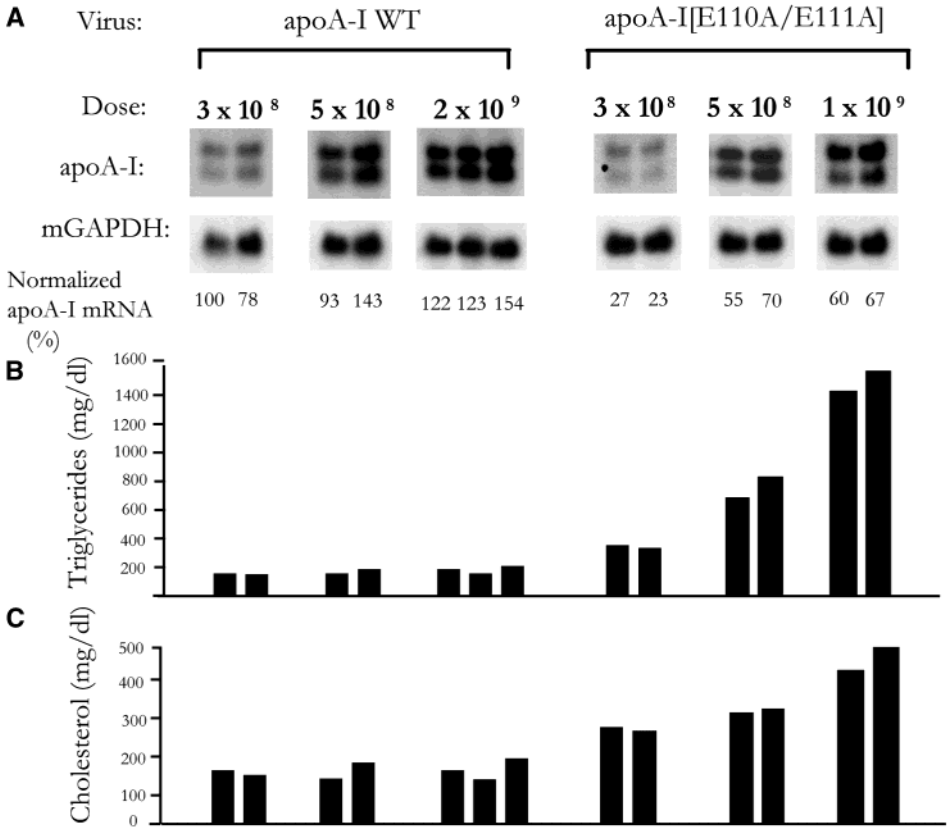

FIGURE 2: Correlation of hepatic apoA-I mRNA levels with plasma lipid levels of individual mice infected with adenoviruses expressing the WT apoA-I and the apoA-I[E110A/E111A] mutant. Panel A shows a representative autoradiogram of Northern blot analysis of total RNA isolated from livers of individual mice infected with the indicated dose of the recombinant adenoviruses expressing WT apoA-I or the apoA-I[E110A/E111A] mutant. Panel B shows the cholesterol levels of individual mice expressed in mg/dL. Panel C shows the triglyceride levels of the individual mice expressed in mg/dL.

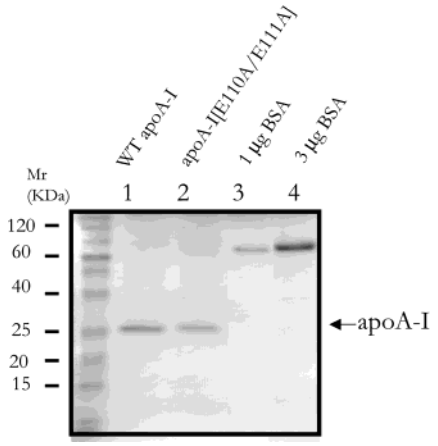

FIGURE 3: Expression of WT apoA-I and the apoA-I[E110A/E111A] mutant in cultures of HTB-13 cells following infection with the corresponding recombinant adenoviruses. SDS−PAGE analysis of medium obtained from HTB-13 cells in 100 mm dishes infected with adenoviruses expressing the WT apoA-I and the apoA-I[E110A/E111A] as described in Experimental Procedures is presented. An aliquot of 15 μL of serum-free culture medium was analyzed. The first lane contains protein markers of different M_r, as indicated. Lanes 3 and 4 contain 1 and 3 μg of BSA, respectively. It was estimated that the infected cultures (5×10^6 cells) secreted approximately 100 and 60 μg/mL WT apoA-I and the apoA-I[E110A/E111A] mutant, respectively, over 24 h of incubation.

the mutant apoA-I were distributed exclusively in the VLDL region. As expected, the VLDL triglyceride levels in mice expressing the WT apoA-I were very low (Figure 4B). Analysis of plasma apoA-I levels by sandwich ELISA confirmed the distribution of WT apoA-I in the HDL2 and HDL3 regions and the apoA-I[E110A/E111A] mutant in the HDL3 and to a lesser extent in the VLDL and LDL regions (Figure 4C).

Effect of the apoA-I[E110A/E111A] Mutation on VLDL Triglyceride Secretion. The rate of hepatic VLDL triglyceride secretion in the plasma of apoA-$I^{-/-}$ mice was determined following injection of Triton WR1339 4 days after the infection with the recombinant adenoviruses expressing the WT and the mutant apoA-I. It was found that the rate of VLDL triglyceride secretion was similar for the mice infected with adenoviruses expressing either the WT or the mutant apoA-I forms or for uninfected control mice (data not shown).

Effect of the apoA-I[E110A/E111A] Mutation on the Distribution of apoA-I in Different Lipoproteins, the Apoprotein Composition of VLDL, and the Size and Shape of HDL. Analysis of the distribution of apoA-I following density gradient ultracentrifugation of plasma showed that the WT apoA-I was predominantly distributed in the HDL2 and HDL3 region with small amounts found in the lower density regions (Figure 5A). Consistent with the FPLC data, the peak concentration of the mutant apoA-I was in the HDL3 region. In addition, higher concentrations of the mutant apoA-I were distributed in the VLDL and IDL region as compared to the WT apoA-I (Figure 5B). Similar results were obtained by analysis of the apoA-I distribution following equilibrium density gradient ultracentrifugation of plasma (data not shown).

Analysis of the apolipoprotein composition of the VLDL-containing fraction showed that infection of mice with

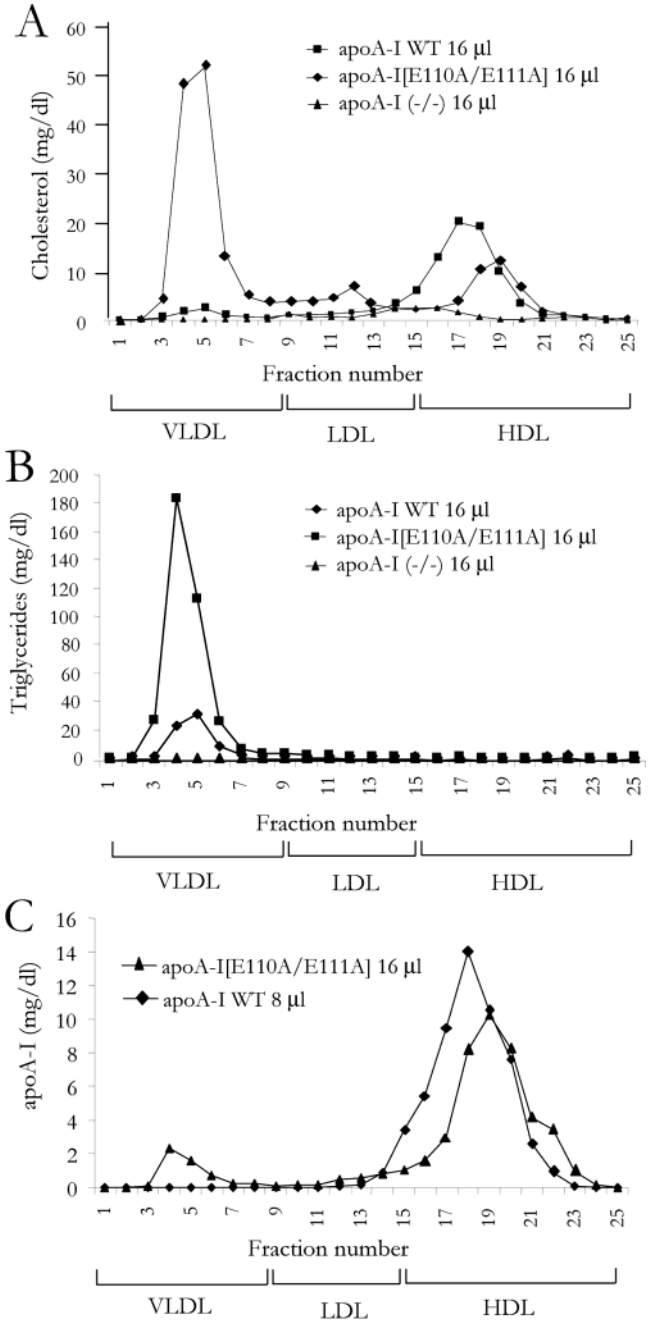

FIGURE 4: FPLC profiles of cholesterol, triglycerides, and apoA-I in plasma of apoA-I-deficient mice infected with recombinant adenoviruses expressing the WT apoA-I or the apoA-I[E110A/E111A] mutant. Plasma samples were obtained from mice infected with 1×10^9 pfu of the recombinant adenoviruses expressing the WT apoA-I or the apoA-I[E110A/E111A] mutant 4 days postinfection. The samples were fractionated by FPLC, and then the cholesterol (panel A), triglycerides (panel B), and apoA-I (panel C) levels of each FPLC fraction were determined as described in Experimental Procedures.

recombinant adenoviruses expressing the apoA-I[E110A/E111A] mutant was associated with increase in apoB-48 and decrease in apoE and apoCII (Figure 5C).

Analysis by electron microscopy of the HDL formed showed that both the WT and the mutant apoA-I formed spherical particles (Figure 5D,E), whereas apoA-I of the fraction of $d > 1.21$ g/mL did not contain any lipoprotein particles (data not shown). The average size of the HDL particles that contained the mutant apoA-I[E110A/E111A]

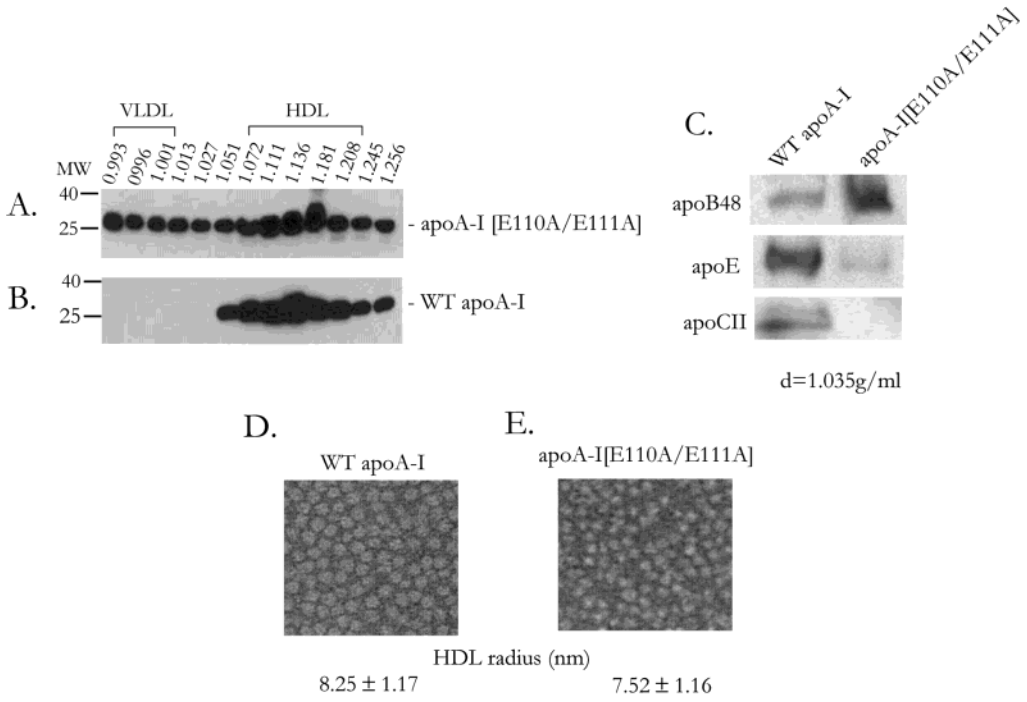

FIGURE 5: SDS−PAGE analysis of fractions of plasma that was separated by density gradient ultracentrifugation and EM pictures of HDL fractions**.** Plasma was isolated from apoA-I-deficient mice 4 days postinfection with adenoviruses expressing WT apoA-I (panel A) or the apoA-I[E110A/E111A] mutant (panel B) and was separated by density gradient ultracentrifugation as described in Experimental Procedures. The densities of the fraction are indicated on the top of the figure. Fractions with the highest apoA-I concentration, as well as the $d > 1.21$ g/mL fractions, were analyzed by electron microscopy. Panel C, assessment of the apoprotein composition of VLDL/IDL isolated from plasma of mice infected with WT apoA-I and apoA-I[E110A/E111A] by Western blotting. Polyclonal antibodies to mouse apoB, apoE, and apoCII were used for detection as described in Experimental Procedures. EM pictures of HDL fractions obtained from mice infected with adenoviruses expressing WT apoA-I (panel D) or the apoA-I[E110A/E111A] mutant (panel E) are presented. The photomicrographs were taken at 75,000× magnification and enlarged 3 times. The size of the lipoprotein particles is indicated underneath panels D and E. The fractions from the plasma of mice expressing WT apoA-I were diluted 3 times.

appear to be smaller as compared with particles containing the WT apoA-I. However, the difference did not reach statistical significance (Figure 5D,E). Two-dimensional gel electrophoresis showed that both the WT and the mutant apoA-I had a similar pattern of preβ1 and of αHDL particles (data not shown).

In Vitro Inhibition of the Activity of Lipoprotein Lipase by apoA-I and Diminished Hydrolysis of VLDL Obtained from Mice Expressing the apoA-I[E110A/E111A]. We have analyzed the ability of apoA-I to inhibit the activity of lipoprotein lipase in vitro. Approximately 50% inhibition was obtained at apoprotein concentrations of ~60 μg/mL with both the WT apoA-I and the apoA-I[E110A/E111A] mutant (Figure 6A). Consistent with this finding, the VLDL/IDL fraction obtained from the plasma of mice infected with the adenovirus expressing the apoA-I[E110A/E111A] mutant was hydrolyzed less efficiently than the VLDL/IDL fraction obtained from mice infected with the adenovirus expressing the WT apoA-I, mainly due to the reduction in the $V_{max,app}$ of the reaction (Figure 6B).

Coexpression of apoA-I[E110A/E111A] and Lipoprotein Lipase Corrects the apoA-I-Induced Hypertriglyceridemia in apoA-I$^{-/-}$ Mice. The induction of dyslipidemia characterized by severe hypertriglyceridemia and increased plasma cholesterol levels in apoA-I-deficient mice could be the result of the insufficiency of the circulating lipoprotein lipase activity, apoCII, or both. To test these possibilities, apoA-I-deficient mice were infected with either 1×10^9 pfu of the adenovirus-expressing apoA-I[E110A/E111A] alone or a mixture of 1×10^9 pfu of each adenovirus expressing the mutant apoA-I and the WT or an inactive form of human lipoprotein lipase (*20*, *22*). This analysis showed that coinfection with the adenovirus expressing the WT lipoprotein lipase and the mutant apoA-I corrected the hypertriglyceridemia (Figure 7A). In contrast coinfection with the adenovirus expressing a mutant form of the lipoprotein lipase having a S132T substitution and the helix 4 mutant of apoA-I corrected only partially the hypertriglyceridemia 4 days postinfection (Figure 7A). The finding indicates that in mice expressing apoA-I[E110A/E111A], the endogenous lipoprotein lipase activity may be rate-limiting for the lipolysis, clearance of VLDL, or both. The total plasma cholesterol levels were not affected significantly by coinfection with LPL 2 and 3 days postinfection and were slightly decreased 4 days postinfection (Figure 7B).

Physicochemical Analysis of the apoA-I[E110A/E111A] Mutant. The α-helical content of the WT apoA-I and the apoA-I[E110A/E111A] in solution and on rHDL was estimated from the normalized far-UV CD spectra. For the lipid-free state, it was found that the mutation results in ~7% reduction in the protein α-helical content, which corresponds to the loss of ~18 residues in the helical conformation (Table 3, section A). Far-UV CD analysis of rHDL containing the WT apoA-I or apoA-I[E110A/E111A] mutant showed that in the lipid-bound state, the mutation results in a reduction in the α-helical content of apoA-I by ~4%, which corresponds to the loss of ~10 residues in the helical conformation of the lipid-bound protein (Table 3, section B). Thus, the E110A/E111A mutation leads to unfolding of α-helical segment(s) in apoA-I in both the lipid-free state and on rHDL

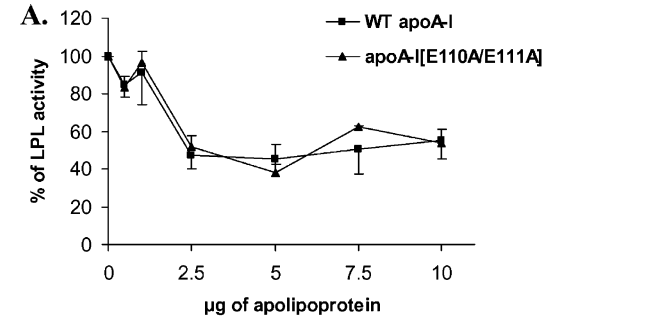

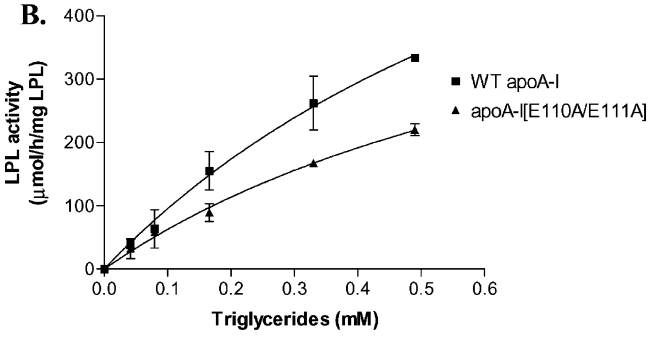

	WT apoA-I	apoA-I[E110A/E111A]
Km_{app} (mM)	0.92±0.22	0.87±0.23
$Vmax_{app}$ (µmol/h/mg of LPL)	973±170	610±112*

FIGURE 6: Effect of apoA-I on the in vitro lipolysis of triglycerides emulsions and VLDL. Panel A shows the inhibition of the activity of lipoprotein lipase by increasing concentrations of WT apoA-I and the apoA-I[E110A/E111A] mutant. The enzymatic reactions were performed as described in Experimental Procedures. The initial velocity of the enzymatic reaction in the presence of 0.7 mM triglycerides, which equals the $K_{m,app}$ of LPL, was set as the 100% value. Panel B shows a diagram of initial velocity of VLDL/IDL hydrolysis vs the concentration of the VLDL/IDL triglycerides. Experiments were performed as described in Experimental Procedures. The kinetic parameters of the enzymatic reaction were calculated using the Prism software. The ∗ indicates significant differences, $p < 0.05$.

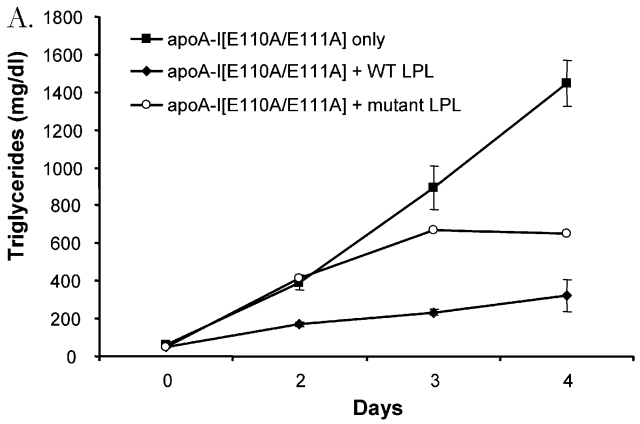

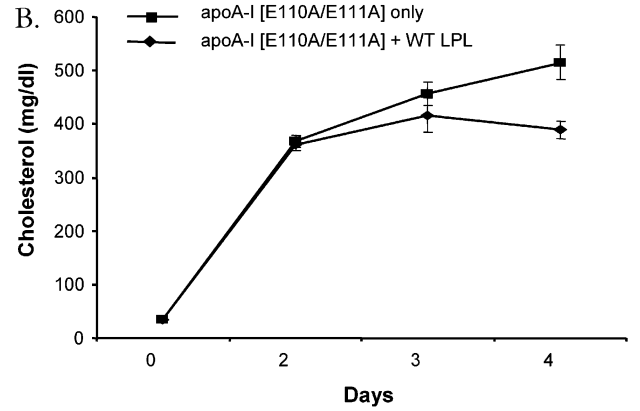

FIGURE 7: Cholesterol and triglycerides plasma levels in apoA-I-deficient mice infected with recombinant adenoviruses expressing the apoA-I[E110A/E111A] mutant alone or a combination of the apoA-I mutant and WT or mutant human lipoprotein lipase. Plasma samples were obtained from mice infected with 1×10^9 pfu of the recombinant adenovirus expressing the apoA-I[E110A/E111A] mutant alone or in combination with 1×10^9 pfu of an adenovirus expressing the WT or an inactive form of lipoprotein lipase (having a S132T substitution) 2, 3, and 4 days postinfection. Triglyceride (panel A) and cholesterol (panel B) levels were determined as described in Experimental Procedures.

particles. Furthermore, by comparison of the α-helical content of lipid-free and lipid-bound apoA-I, it appears that the loss of ∼18 residues in the α-helical conformation of lipid-free mutant apoA-I was not fully restored by binding to lipids.

The thermal unfolding curves for lipid-free apoA-I monitored by ellipticity at 222 nm, $\Theta_{222}(T)$, are shown in Figure 8A, the corresponding van't Hoff plots are shown in the insert, and the values of the melting temperature, T_m, and the effective enthalpy, ΔH_v, determined from the van't Hoff analysis are given in Table 3, section A. The apoA-I[E110A/E111A] mutant shows a ∼5 °C decrease in T_m, indicating a destabilizing effect of the mutation, and a ∼19 kcal/mol reduction in ΔH_v, suggesting significantly lower cooperativity of the thermal transition of the mutant protein compared to the WT apoA-I. The shape of the melting curve for the apoA-I[E110A/E111A] also suggests lower cooperativity of unfolding.

The GdnHCl-induced unfolding curves for lipid-free proteins are shown in Figure 8B, the free energy of denaturation ΔG_D of apoA-I as a function of GdnHCl concentration is shown in the insert, and the conformational stability, ΔG_D° (the free energy of denaturation at zero GdnHCl), the midpoint of chemical denaturation, $D_{1/2}$, and m values determined from the plots are listed in Table 3, section A. The analysis of GdnHCl-induced unfolding of lipid-free apoA-I showed that the apoA-I[E110A/E111A] mutant had a ∼1.1 kcal/mol reduction in ΔG_D°, indicating a large destabilizing effect of the two point amino acid substitutions. It also shows reduction in the m value by ∼1.0 kcal/(moles of apoA-I × moles of GdnHCl), suggesting lower cooperativity of the chemical unfolding of the mutant protein as compared to the WT apoA-I.

The GdnHCl-induced denaturation of apoA-I bound to lipids on rHDL was monitored by ellipticity at 222 nm after the incubation of aliquots of rHDL with various GdnHCl concentrations for 72 h to allow the proteins to achieve complete denaturation (*41*). The GdnHCl-induced denaturation curves for apoA-I on rHDL are shown in Figure 8C, the insert shows the effect of GdnHCl concentration on the free energy of denaturation, ΔG_D, and the thermodynamic parameters of the chemical denaturation, ΔG_D°, m, and $D_{1/2}$, are listed in Table 3, section B. The analysis of GdnHCl-induced denaturation of lipid-bound apoA-I showed that the apoA-I[E110A/E111A] mutant had a small but significant reduction in the conformational stability, ΔG_D° (by ∼0.5 kcal/

Table 3: α-Helical Content and Thermodynamic Parameters Determined by Far-UV CD

(A) Lipid-Free WT apoA-I and Mutant apoA-I[E110A/E111A]

protein	α-helix[a] (%)	# residues in protein	# residues in helix[b]	T_m,[c] °C	ΔH_v,[c] kcal/mol	$\Delta G_D°$,[d] kcal/mol	m,[d] kcal/(moles of apoA-I × moles of GdnHCl)	$D_{1/2}$,[d] M
WT apoA-I	∼59	249	∼147	59 ± 1	49 ± 1	3.1 ± 0.3	3.0 ± 0.2	1.0 ± 0.05
apoA-I[E110A/E111A]	∼52	249	∼129 (−18)	54 ± 0.5[e]	30 ± 1[e]	2.0 ± 0.2[f]	2.0 ± 0.2[f]	1.0 ± 0.00

(B) apoA-I in rHDL Made with apoA-I[E110A/E111A] and WT apoA-I

rHDL	α-helix[a] (%)	# residues in protein	# residues in helix[b]	$\Delta G_D°$,[d] kcal/mol	m,[d] kcal/(moles of apoA-I × moles of GdnHCl)	$D_{1/2}$,[d] M
WT apoA-I	∼67	249	∼167	4.1 ± 0.3	1.8 ± 0.1	2.3 ± 0.0
apoA-I[E110A/E111A]	∼63	249	∼157 (−10)	3.6 ± 0.1[f]	1.5 ± 0.05[f]	2.3 ± 0.1

[a] Estimated from the value Θ_{222} at 25 °C (*37*); systematic error of the estimation is ±3%; statistical error is within ±1−3%. [b] Determined by multiplying the number of residues in the protein by its α-helical content. Values in parentheses show changes in the number of residues as compared to WT apoA-I. [c] Melting temperature, T_m, and effective enthalpy, ΔH_v, of thermal unfolding were determined from van't Hoff analysis of the melting curves monitored by ellipticity at 222 nm. [d] Conformational stability, $\Delta G°_D$, midpoint of chemical denaturation, $D_{1/2}$, and m values were determined by the linear extrapolation method from CD-monitored chemical unfolding curves. [e] Significance of differences from the value for WT apoA-I is $p < 0.005$. [f] Significance of differences from the value for WT apoA-I is $p < 0.05$.

mol), and the m value (by ∼0.3 kcal/(moles of apoA-I × moles of GdnHCl)). Thus, the two point mutations destabilize both lipid-free and lipid-bound apoA-I, although the destabilizing effect of the mutations on the protein conformation in lipid free state is bigger than that on the protein on rHDL.

Binding of the amphipathic dye ANS to the WT apoA-I and the apoA-I[E110A/E111A] mutant was studied to find out whether the mutation affects the exposure of hydrophobic surfaces or cavities of lipid-free apoA-I. It was found that the intrinsic fluorescence of the amphipathic dye ANS is increased upon binding to hydrophobic surfaces or cavities, while the water-phase dye does not contribute to the emission (*42*). ANS fluorescence spectra were recorded in the presence of 50 μg/mL bovine serum albumin, WT apoA-I, apoA-I[E110A/E111A], or carbonic anhydrase, or in buffer alone. In the phosphate buffer, ANS has a very low quantum yield and maximum of fluorescence emission of 515 nm (Figure 8D). In the presence of WT apoA-I, the ANS emission spectrum shows a ∼3-fold increase in intensity and a 35 nm blue shift (from 515 to 480 nm) in its wavelength of maximum emission. There is an even more substantial increase in fluorescence intensity (∼4.5-fold) and a bigger (∼38 nm) blue shift (from 515 to 477 nm) in the presence of the apoA-I[E110A/E111A]. This indicates that the mutant apoA-I binds more ANS molecules as compared to WT apoA-I, presumably due to increased exposure of hydrophobic surfaces in the mutant protein. The "negative control", carbonic anhydrase, had no significant effect on ANS fluorescence, consistent with the compact folding of this globular protein. In contrast, the "positive control", bovine serum albumin, induced the largest (∼6-fold) enhancement in ANS fluorescence spectra, consistent with its known ability to bind hydrophobic molecules.

Kinetics of Association of apoA-I with DMPC Liposomes. The kinetics of association of lipid-free WT apoA-I and apoA-I[E110A/E111A] with DMPC multilamellar vesicles was followed by the decrease in the turbidity at 325 nm, which reflects the formation of DMPC−apoA-I complexes (Figure 8E). It was found that both WT apoA-I and apoA-I[E110A/E111A] have a similar rate of association with DMPC liposomes.

Formation of Discoidal POPC−apoA-I Particles by the WT apoA-I and the apoA-I[E110A/E111A]. The sodium cholate dialysis method was used to generate discoidal particles with the WT apoA-I and the apoA-I[E110A/E111A]-form (*26*). The rHDL particles generated contained either unlabeled or both unlabeled and ^{14}C-labeled cholesterol. Unlabeled particles were used for electron microscopy and SR-BI-mediated cholesterol efflux assays, while labeled particles were used for LCAT assays. The electron micrographs showed that particles formed with the WT or the mutant apoA-I form the typical "rouleaux", indicating that they are discoidal and have the thickness of a phospholipid bilayer (data not shown).

Functional Analyses of WT apoA-I and Mutant apoA-I[E110A/E111A] Forms: (i) Activation of LCAT. The LCAT activation potential of the apoA-I[E110A/E111A] was examined using LCAT purified from the culture medium of human astrocytoma HTB-13 cells infected with an adenovirus that expresses the human LCAT (*21*). WT and mutant apoA-I forms used for the generation of rHDL particles were isolated from the HTB-13 cells following adenovirus infection as described in Experimental Procedures.

The LCAT activity was assayed as the rate of production of labeled cholesteryl esters from the rHDL particles. The kinetic parameters of LCAT activation were determined from the initial velocities of cholesterol esterification of the rHDL substrate at various apoA-I concentrations. The apparent catalytic efficiency ($V_{max,app}/K_{m,app}$) of the enzyme using rHDL particles containing the apoA-I[E110A/E111A] mutant was reduced to approximately 37% of that using rHDL particles containing the WT apoA-I. This decrease was accounted for by a similar reduction in the $V_{max,app}$ (Figure 9A).

(ii) ABCA1-Mediated Efflux of Cellular Cholesterol in HEK293 Cells Transfected with an ABCA1 Expression Plasmid. HEK293 EBNA-T cells were transfected with empty vector or an ABCA1 expression plasmid for 16 h, as described in Experimental Procedures. Following transfection, the cells were labeled with [^{3}H]cholesterol for 24 h and then incubated with or without 1 μM lipid-free WT apoA-I or apoA-I[E110A/E111A] for 4 h. Media and cells were collected separately, and the radioactivity in the media, as well as in the cell lysate, was determined as described in Experimental Procedures. The percent of [^{3}H]cholesterol efflux represents the amount of the radioactivity released in the medium divided by the total radioactivity present in the

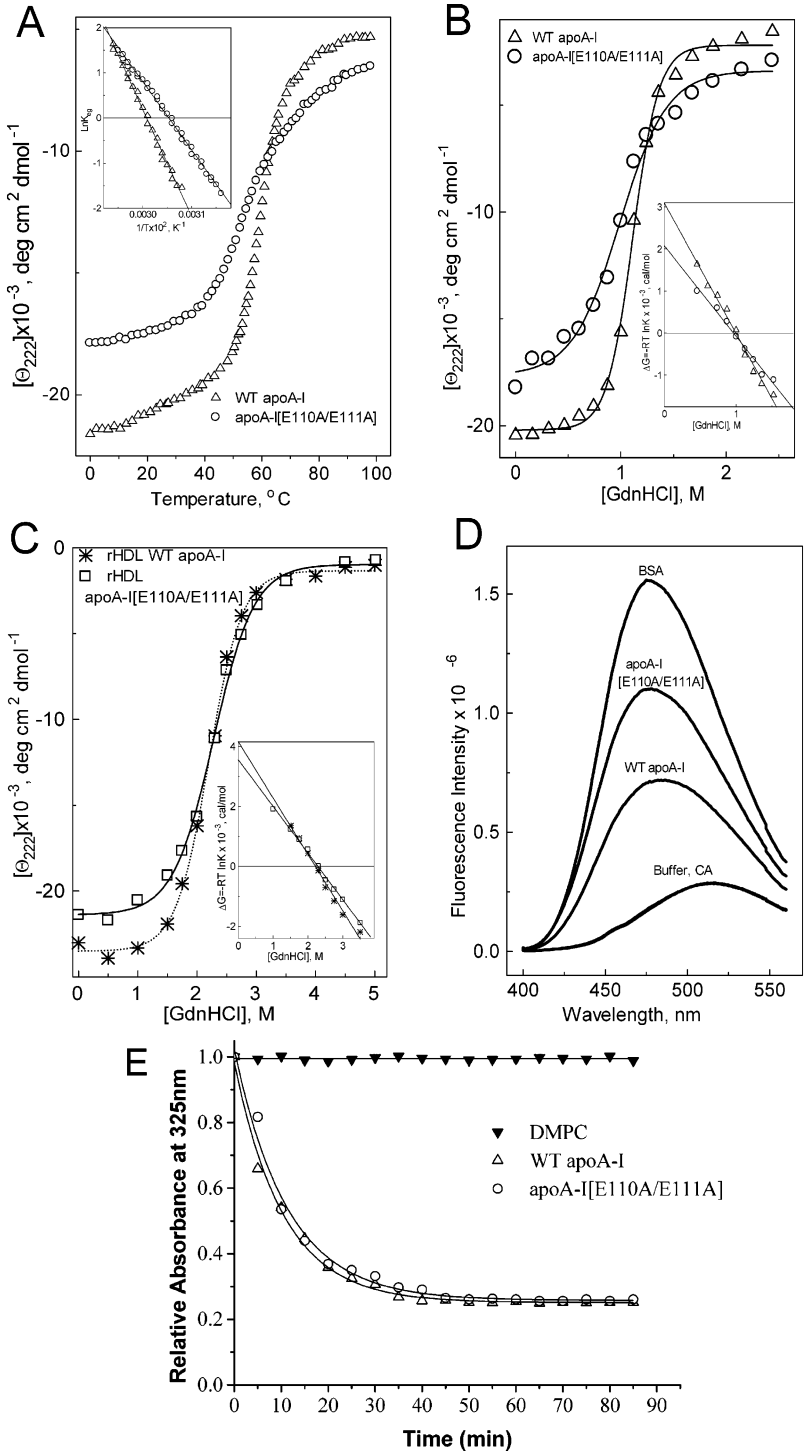

FIGURE 8: Physicochemical properties of WT apoA-I and apoA-I[E110A/E111A] mutant. Thermal unfolding (panel A) and denaturant-induced unfolding (panel B) of the lipid-free WT apoA-I and the apoA-I[E110A/E111A] mutant was monitored by the ellipticity at 222 nm. The inset in panel A shows the van't Hoff plots (ln K_{eq} versus $1/T$) derived from the corresponding thermal unfolding curves. Denaturant-induced unfolding (panel C) of WT apoA-I and the apoA-I[E110A/E111A] mutant on rHDL particles was monitored by the ellipticity at 222 nm. The insets in panels B and C show the free energy of denaturation, ΔG, as a function of GdnHCl concentration. The symbols in panels A−C indicate the lipid-free WT apoA-I (△), the lipid-free apoA-I[E110A/111A] mutant (○), the lipid-bound WT apoA-I (∗), and the lipid-bound apoA-I[E110A/E111A] (□). Panel D shows ANS fluorescence spectra obtained in the presence of 50 μg/mL bovine serum albumin (BSA), WT apoA-I, apoA-I[E110A/E111A], carbonic anhydrase (CA), or buffer alone. Spectra were recorded in 10 mM phosphate buffer (pH 8) using 5 nm excitation and 2.5 nm emission slit widths. Fluorescence was excited at wavelength of 395 nm, and emission was scanned from 400 to 560 nm. Panel E shows the kinetics of DMPC association of WT apoA-I and apoA-I[E110A/E111A] with multilamellar DMPC vesicles monitored by turbidity changes over time at 24 °C. Experiments were performed as described in Experimental Procedures. The symbols in panel E are the same as those in panels A and B.

culture medium and the cell lysate. It was found that the ABCA1-mediated cholesterol efflux was similar for the WT apoA-I and the apoA-I[E110A/E111A] mutant (Figure 9B).

(iii) SR-BI-Mediated Cholesterol Efflux. POPC/cholesterol/apoA-I discoidal rHDL particles with either wild-type apoA-I or the mutant apoA-I[E110A/E111A] were prepared by the

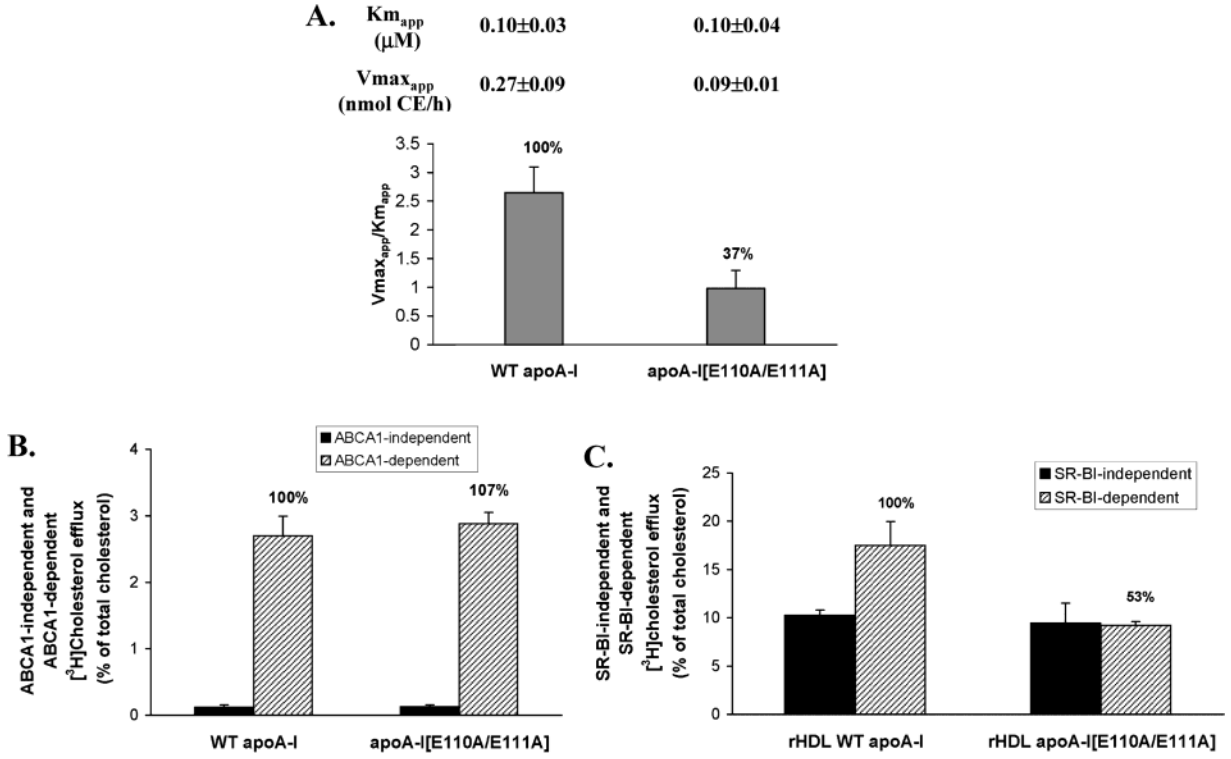

FIGURE 9: Functional analyses of apoA-I in lipid-bound or lipid-free form. Panel A shows activation of LCAT by rHDL containing WT apoA-I and the apoA-I[E110A/E111A] mutant. The substrate particles containing POPC/cholesterol and [^{14}C]cholesterol/apoA-I/sodium cholate at a starting molar ratio of 100:10:1:100 were prepared as described under Experimental Procedures. Each LCAT assay contained final apoA-I concentrations ranging from 5×10^{-8} to 2.5×10^{-6} M and sufficient LCAT concentration to keep the extent of cholesterol esterification below 15%. The reaction was carried out for 30 min at 37 °C, and the conversion of [^{14}C]cholesterol to [^{14}C]cholesteryl ester was determined by extraction of the lipids of the incubation mixture followed by thin-layer chromatography as described under Experimental Procedures. The cholesterol esterification rate was expressed as nanomoles of cholesteryl ester formed per hour. The rate of cholesteryl ester formation was plotted against the apoA-I concentration, the data were fitted to Michaelis−Menten kinetics, and the apparent K_m and V_{max} values were calculated. The catalytic efficiency, $V_{max,app}/K_{m,app}$ of the enzyme using rHDL containing either WT or the mutant apoA-I was calculated and is shown in panel A. Values are the means ± SD from three independent experiments performed in duplicate. Panel B shows the effect of the E110A/E111A mutation in apoA-I on ABCA1-mediated efflux of cellular cholesterol in HEK293 EBNA-T cells transfected with an ABCA1 expression plasmid. Cells were transfected with empty vector (mock) or with ABCA1 plasmid for 16 h, labeled with 0.5 μCi/mL [^{3}H]cholesterol for 24 h in DMEM (high-glucose) containing 10% (v/v) FBS, and then incubated with 1 μM lipid-free WT and mutant apoA-I form in 0.5 mL DMEM (high-glucose) containing 0.2% (w/v) fatty acid-free BSA for 4 h at 37 °C. Media and cells were collected separately, and the radioactivity in the media, as well as in the cell lysate, was determined as described in Experimental Procedures. The percent of [^{3}H]cholesterol efflux represents the amount of the radioactivity released in the medium divided by the total radioactivity present in the culture medium and the cell lysate. Black bars show the percent of ABCA1-independent cholesterol efflux. Shaded bars show the percent of the net ABCA1-mediated [^{3}H]cholesterol efflux, calculated as the difference in percent of cholesterol efflux between ABCA1-transfected and mock-transfected cells. The numbers on top of the bars represent the cholesterol efflux relative to the WT control set to 100%. Values are the means ± SD from three independent experiments performed in duplicate. Panel C shows the effect of the E110A/E111A mutation of apoA-I on rHDL-dependent cholesterol efflux from control cells (ldlA-7) and cells expressing SR-BI (ldlA[mSR-BI]). The ldlA[mSR-BI] and ldlA-7 cells were plated at 200 000 cells/well in 6-well dishes, labeled with [^{3}H]cholesterol for 48 h in Ham's F-12 medium containing 10% (v/v) NCLPDS, washed, incubated in Ham's F-12 medium containing 1% (w/v) fatty-acid-free BSA for 24 h, washed, and incubated for 45 min at 37 °C with 1 mL of Ham's F-12 medium, as described under Experimental Procedures. The medium was then aspirated and replaced with 1 mL of Ham's F-12 medium containing 28 μg/mL protein (1 μM) of rHDL prepared with WT apoA-I or apoA-I[E110A/E111A]. After incubation at 37 °C for various time points, [^{3}H]cholesterol released to the media from ldlA-7 cells or ldlA[mSR-BI] cells was measured as described under Experimental Procedures. At the end of the incubation period, the cells were lysed, and the radioactivity in the cell lysate was measured. The percent of [^{3}H]cholesterol efflux represents the amount of the radioactivity released in the medium divided by the total radioactivity present in the culture medium and the cell lysate. The percent [^{3}H]cholesterol efflux after 4 h incubation is shown in panel C. Black bars show the percent of SR-BI-independent cholesterol efflux. Shaded bars show the percent of the net SR-BI-mediated [^{3}H]cholesterol efflux, calculated as the difference in percent of cholesterol efflux between ldlA[mSR-BI] and ldlA-7 cells. The numbers on top of the bars represent the cholesterol efflux relative to the WT control set to 100%. Values are the means ± SD from three independent experiments performed in duplicate.

sodium cholate method (*26*). The particles containing the WT and the mutant apoA-I had similar sizes with apparent diameters of 96 Å (not shown). These rHDL preparations were used to determine the time course of cholesterol efflux over a 6 h period from control ldlA-7 cells that express almost no SR-BI (*31*, *32*, *43*) or the ldlA[mSR-BI] cells that express high levels of wild-type murine SR-BI as a consequence of stable transfection with a mSR-BI expression vector (*31*, *44*). It was found that efflux rates of [^{3}H]-cholesterol from control ldlA-7 cells to the rHDLs (28 μg/mL protein, 1 μM) were similar. In contrast, efflux rates from ldlA[mSR-BI] cells to rHDL, which represents the total cholesterol efflux, were greater than the rates for the control ldlA-7 cells. The differences between the rates measured in the transfected (ldlA[mSR-BI]) and untransfected control (ldlA-7) cells represent SR-BI-dependent efflux. To simplify the analysis, the extent of efflux mediated by rHDLs containing the WT apoA-I after 4 h incubation at 37 °C was

defined as 100%. Compared with the rHDL containing WT apoA-I, the SR-BI-mediated efflux capacity of rHDLs containing the apoA-I[E110A/E111A] mutant was reduced to 53% (Figure 9C). The findings indicate that the substitutions of alanine for glutamate 110 and 111 in apoA-I reduced the capacity of the rHDLs to mediate SR-BI-dependent cholesterol efflux.

DISCUSSION

Background. Mutations or alterations in the plasma levels of various proteins that participate in HDL metabolism, such as LCAT, CETP, HL, SR-BI, ABCA1, endothelial lipase, and lipoprotein lipase, may have adverse effects on HDL concentrations and functions (*45*−*56*). Previous studies have shown that lack of HDL in patients with Tangier disease is associated with moderate hypertriglyceridemia (*16*, *57*). Statistically significant association between moderate hypertriglyceridemia has been reported in the carriers of apoA-I Milano, as well as the male carriers of apoA-IΔLys107 (*13*−*15*). These findings indicate that apoA-I and HDL functions may be required for plasma triglyceride homeostasis.

With the exception of defects in lipoprotein lipase and apoCII (*54*, *58*), the molecular etiology of most forms of hypertriglyceridemia in humans remains unclear. Recently it has been shown that hypertriglyceridemia can be induced by overexpression of apoCIII, apoCII, apoCI, apoA-II, and apoE in transgenic mice (*59*−*64*), by adenovirus-mediated gene transfer (*27*, *65*), or by inactivation of the apoA-V gene in mice (*66*). In addition, in humans, plasma apoE and apoCIII levels correlate with plasma triglyceride levels (*67*, *68*).

Changes in the Structure of Lipid-Free and Lipid-Bound apoA-I Induced by the E110A/E111A Mutation. The α-helical content of WT and mutant apoA-I in the lipid-free state and on the rHDL particles was estimated from the normalized far-UV CD spectra. It was found that compared to the WT apoA-I, the apoA-I[E110A/E111A] had approximately 18 fewer residues in the α-helical conformation in the lipid-free state and 10 fewer residues in the α-helical conformation in the lipid-bound state (Table 3). In addition, the lipid-free apoA-I[E110A/E111A] mutant showed greatly reduced chemical and thermal stability and cooperativity of unfolding as compared to the WT apoA-I. Similarly, chemical denaturation of WT and mutant apoA-I on rHDL particles showed that in the lipid-bound state the mutant apoA-I also had slightly reduced chemical stability and cooperativity of unfolding as compared to the WT apoA-I. ANS fluorescence measurements in the presence of the WT apoA-I and the apoA-I[E110A/E111A] mutant indicated that, consistent with molten globular-like structure of apoA-I (*69*, *70*), both the WT and the mutant apoA-I forms possess hydrophobic surfaces exposed to the solvent. However, the comparative analysis showed that hydrophobic residues in the mutant apoA-I[E110A/E111A] are more accessible to solvent compared with those of WT apoA-I. The finding suggests a looser structure of the mutant protein that is only weakly stabilized by tertiary interactions. This interpretation is consistent with the significantly lower stability and unfolding cooperativity of the mutant protein demonstrated by the thermal and chemical denaturation experiments.

Changes in the in Vitro and in Vivo Functions of apoA-I as a Result of the E110A/E111A Mutation. ApoA-I is the major protein of HDL and plays a crucial role in the synthesis, structure, and function of HDL (*1*). It is generally believed that the initial functional interactions of lipid-free apoA-I with the ABCA1 transporter contribute to the lipidation of apoA-I. The particles formed through a series of intermediates give rise to discoidal HDL particles, which are subsequently converted to spherical particles by the action of LCAT (*6*, *9*, *71*−*74*). Discoidal and spherical HDL particles can interact with the HDL receptor (SR-BI). These interactions are associated with selective lipid uptake and net efflux of cellular cholesterol in vitro (*10*, *11*, *31*). Finally, cholesteryl esters in humans can be transferred from HDL to VLDL/LDL with reciprocal transfer of triglycerides by the action of cholesteryl ester transfer protein (CETP); however, mice lack CETP activity (*75*, *76*). The striking finding of the current study is that adenovirus-mediated transfer of apoA-I[E110A/E111A] in apoA-I-deficient mice is associated with severe hypertriglyceridemia and increased plasma cholesterol levels as compared to mice infected with WT apoA-I. These observations link directly the structural changes in apoA-I with malfunction of apoA-I, HDL, or both that may be responsible for the induction of hypertriglyceridemia.

We have performed a series of functional assays to identify changes in the in vitro and in vivo functions of apoA-I that could explain the induction of hypertriglyceridemia by the mutant apoA-I form.

Cholesterol efflux studies in ABCA1-transfected HEK293 EBNA cells showed that both the WT and the apoA-I[E110A/E111A] mutant have similar ability to promote ABCA1-mediated cholesterol efflux. This finding is consistent with the similar ability of the WT and the mutant apoA-I form to solubilize multilamellar DMPC vesicles in vitro and to promote formation of normal populations of preβ1 and αHDL particles in vivo.

The next question was the ability of the apoA-I to activate LCAT. This analysis showed that the apparent catalytic efficiency ($V_{max,app}/K_{m,app}$) of the enzyme using rHDL containing the apoA-I[E110A/E111A] was 37% of that using rHDL containing the WT apoA-I. Previous studies using synthetic peptides had suggested that residue E111 of the human apoA-I might be critical for the activation of LCAT in vitro (*18*). Nevertheless, these levels of LCAT activation by this apoA-I mutant were sufficient to promote formation of spherical αHDL particles in vivo, as determined by EM analysis of HDL obtained from mice infected with the WT or the mutant apoA-I form. The combined observations listed above suggest that the apoA-I[E110A/E111A] mutation of apoA-I did not affect the biogenesis of HDL particles in vivo. Based both on electron microscopy (EM) and on FPLC profiles, the size of the HDL particles derived from mice expressing the mutant apoA-I appeared smaller compared with the particles obtained from mice expressing the WT apoA-I. This reduction in size may be related to the loss of α-helical structure in the apoA-I[E110A/E111A] mutant as compared to the WT apoA-I.

Cholesterol efflux studies using a cell line expressing the mouse SR-BI [ldlA(mSR-BI)] showed that rHDL particles containing apoA-I[E110A/E111A] were 53% as efficient to promote SR-BI-mediated cholesterol efflux compared with particles containing the WT apoA-I. The physiological significance of SR-BI-mediated cholesterol efflux in vivo is

not fully understood. However, it has been shown that homozygous or heterozygous deficiency in SR-BI in mice is associated with increase in HDL size (*45*). On the basis of these data, one would expect that impairment of interaction of HDL with SR-BI in vivo as a result of the E110A/E111A mutation might lead to an increase rather than decrease in the HDL particle size. Thus our findings suggest that the E110A/E111A mutation in apoA-I may not have significant effect on the in vivo interactions of HDL with SR-BI that might account for the observed hypertriglyceridemia.

Potential Mechanism of Hypertriglyceridemia Induced by the E110A/E111A Mutation and Clinical Implications. Analysis of the distribution of apoA-I in different lipoprotein fractions following density gradient ultracentrifugation or FPLC fractionation showed that approximately 15% of apoA-I was distributed in the non-HDL region (i.e., LDL, IDL, and VLDL). This suggests that the apoA-I[E110A/E111A] mutant has increased affinity for the lower density lipoproteins. The tendency of the helix 4 mutant of apoA-I to associate with VLDL was also demonstrated by in vitro density gradient ultracentrifugation experiments in which [^{35}S]-labeled WT or the helix 4 mutant forms of apoA-I were mixed with plasma lipoproteins in the presence of excess VLDL (data not shown). Under these experimental conditions, a small portion of the helix 4 mutant of apoA-I was associated with VLDL and IDL. However, we believe that the in vivo data are more representative of the physiological situation because they represent association of apoA-I with VLDL either prior to or after the secretion of VLDL, whereas the in vitro experiments represent only extracellular association of apoA-I with VLDL and HDL. This raised the possibility that the presence of apoA-I in VLDL, IDL, and LDL hinders the lipolysis of these particles and contributes to hypertriglyceridemia. Consistent with this interpretation, either WT or mutant apoA-I inhibits the activity of mouse LPL in vitro. In addition, in vitro lipolysis of VLDL-containing lipoprotein fractions isolated from the plasma of mice expressing the apoA-I[E110A/E111A] mutant was less efficient than that of VLDL isolated from the plasma of mice expressing the WT apoA-I. Impairment of lipolysis was also tested in vivo by coinfection of mice with adenoviruses expressing apoA-I[E110A/E111A] and either the WT or an inactive form of the human lipoprotein lipase. The treatment with the WT lipoprotein lipase reduced plasma and VLDL triglyceride levels, but it had a smaller effect on plasma cholesterol levels. The treatment with the inactive form of the lipoprotein lipase reduced partially the plasma triglyceride levels 3 and 4 days postinfection as compared with the levels observed in mice infected with the recombinant adenovirus expressing the helix 4 apoA-I mutant. The findings suggest that in mice expressing the apoA-I[E110A/E111A], the activity of lipoprotein lipase is rate-limiting and can account for the observed hypertriglyceridemia in vivo. Factors that can account for the reduction of the activity of lipoprotein lipase is the enrichment of the VLDL/IDL/LDL fraction with apoA-I, combined with reduced concentration of apoCII in these fractions. Furthermore, the reduction of apoE in VLDL/IDL/LDL fractions diminishes direct clearance of triglyceride-rich lipoprotein fractions. The partial reduction of triglyceride levels by the inactive form of lipoprotein lipase may represent previously described receptor-mediated clearance mechanisms (*77*, *78*).

The molecular etiology of common forms of hypertriglyceridemia remains largely unknown. The present study points to the possibility that subtle changes in the structure of apoA-I may underlie conditions of hypertriglyceridemia in humans. It also indicates that apoA-I and HDL may play a crucial but still unidentified role in plasma triglyceride homeostasis. The hypertriglyceridemia induced by apoA-I mutations may be further aggravated by other genetic and environment factors in humans, diabetes, thyroid status, etc. The potential role of apoA-I mutations in hypertriglyceridemia will be addressed in the future by studies in transgenic mice, as well as in selected populations of hypertriglyceridemic patients who may harbor mutations in apoA-I.

ACKNOWLEDGMENT

We thank Dr. Mason Freeman for providing the ABCA1 expression plasmid, Dr. Silvia Santamarina-Fojo for providing the LPL and LCAT adenoviruses, Ms. Gayle Forbes for technical assistance, Dr. David Atkinson for advice on the physicochemical studies, and Ms. Anne Plunkett for typing the manuscript.

NOTE ADDED AFTER ASAP POSTING

This paper was inadvertently published 07/16/04 prior to final corrections being made. The correct version was published 07/23/04.

REFERENCES

1. Zannis, V. I., Kardassis, D., and Zanni, E. E. (1993) Genetic mutations affecting human lipoproteins, their receptors, and their enzymes, *Adv. Hum. Genet. 21*, 145−319.
2. Chroni, A., Liu, T., Gorshkova, I., Kan, H. Y., Uehara, Y., von Eckardstein, A., and Zannis, V. I. (2003) The central helices of apoA-I can promote ATP-binding cassette transporter A1 (ABCA1)-mediated lipid efflux. Amino acid residues 220−231 of the wild-type apoA-I are required for lipid efflux in vitro and high-density lipoprotein formation in vivo, *J. Biol. Chem. 278*, 6719−6730.
3. Laccotripe, M., Makrides, S. C., Jonas, A., and Zannis, V. I. (1997) The carboxyl-terminal hydrophobic residues of apolipoprotein A-I affect its rate of phospholipid binding and its association with high-density lipoprotein, *J. Biol. Chem. 272*, 17511−17522.
4. Liu, T., Krieger, M., Kan, H. Y., and Zannis, V. I. (2002) The effects of mutations in helices 4 and 6 of apoA-I on scavenger receptor class B type I (SR-BI)-mediated cholesterol efflux suggest that formation of a productive complex between reconstituted high-density lipoprotein and SR-BI is required for efficient lipid transport, *J. Biol. Chem. 277*, 21576−21584.
5. Zannis, V. I., and Cohen, J. (2000) Old and new players in the lipoprotein system, *Curr. Opin. Lipidol. 11*, 101−103.
6. Fielding, C. J., and Fielding, P. E. (2001) Cellular cholesterol efflux, *Biochim. Biophys. Acta 1533*, 175−189.
7. Lawn, R. M., Wade, D. P., Garvin, M. R., Wang, X., Schwartz, K., Porter, J. G., Seilhamer, J. J., Vaughan, A. M., and Oram, J. F. (1999) The Tangier disease gene product ABC1 controls the cellular apolipoprotein-mediated lipid removal pathway, *J. Clin. Invest. 104*, R25−R31.
8. Fielding, C. J., Shore, V. G., and Fielding, P. E. (1972) A protein cofactor of lecithin: cholesterol acyltransferase, *Biochem. Biophys. Res. Commun. 46*, 1493−1498.
9. Castro, G. R., and Fielding, C. J. (1988) Early incorporation of cell-derived cholesterol into pre-beta-migrating high-density lipoprotein, *Biochemistry 27*, 25−29.
10. Gu, X., Kozarsky, K., and Krieger, M. (2000) Scavenger receptor class B, type I-mediated [3H]cholesterol efflux to high and low-density lipoproteins is dependent on lipoprotein binding to the receptor, *J. Biol. Chem. 275*, 29993−30001.
11. Ji, Y., Jian, B., Wang, N., Sun, Y., Moya, M. L., Phillips, M. C., Rothblat, G. H., Swaney, J. B., and Tall, A. R. (1997) Scavenger receptor BI promotes high-density lipoprotein-mediated cellular cholesterol efflux, *J. Biol. Chem. 272*, 20982−20985.

12. Stangl, H., Hyatt, M., and Hobbs, H. H. (1999) Transport of lipids from high and low-density lipoproteins via scavenger receptor-BI, *J. Biol. Chem. 274*, 32692−32698.
13. Sirtori, C. R., Calabresi, L., Franceschini, G., Baldassarre, D., Amato, M., Johansson, J., Salvetti, M., Monteduro, C., Zulli, R., Muiesan, M. L., and Agabiti-Rosei, E. (2001) Cardiovascular status of carriers of the apolipoprotein A-I(Milano) mutant: the Limone sul Garda study, *Circulation 103*, 1949−1954.
14. Chiesa, G., Stoltzfus, L. J., Michelagnoli, S., Bielicki, J. K., Santi, M., Forte, T. M., Sirtori, C. R., Franceschini, G., and Rubin, E. M. (1998) Elevated triglycerides and low HDL cholesterol in transgenic mice expressing human apolipoprotein A-I(Milano), *Atherosclerosis 136*, 139−146.
15. Nofer, J. R., von Eckardstein, A., Wiebusch, H., Weng, W., Funke, H., Schulte, H., Kohler, E., and Assmann, G. (1995) Screening for naturally occurring apolipoprotein A-I variants: apo A-I(delta K107) is associated with low HDL-cholesterol levels in men but not in women, *Hum. Genet. 96*, 177−182.
16. Heinen, R. J., Herbert, P. N., and Fredrickson, D. S. (1978) Properties of the plasma very low and low density lipoproteins in Tangier disease, *J. Clin. Invest. 61*, 120−132.
17. Schaefer, E. J., Zech, L. A., Schwartz, D. E., and Brewer, H. B., Jr. (1980) Coronary heart disease prevalence and other clinical features in familial high-density lipoprotein deficiency (Tangier disease), *Ann. Intern. Med. 93*, 261−266.
18. Anantharamaiah, G. M., Venkatachalapathi, Y. V., Brouillette, C. G., and Segrest, J. P. (1990) Use of synthetic peptide analogues to localize lecithin: cholesterol acyltransferase activating domain in apolipoprotein A-I, *Arteriosclerosis 10*, 95−105.
19. Reardon, C. A., Kan, H. Y., Cabana, V., Blachowicz, L., Lukens, J. R., Wu, Q., Liadaki, K., Getz, G. S., and Zannis, V. I. (2001) In vivo studies of HDL assembly and metabolism using adenovirus-mediated transfer of ApoA-I mutants in ApoA-I-deficient mice, *Biochemistry 40*, 13670−13680.
20. Kobayashi, J., Applebaum-Bowden, D., Dugi, K. A., Brown, D. R., Kashyap, V. S., Parrott, C., Duarte, C., Maeda, N., and Santamarina-Fojo, S. (1996) Analysis of protein structure−function in vivo. Adenovirus-mediated transfer of lipase lid mutants in hepatic lipase-deficient mice, *J. Biol. Chem. 271*, 26296−26301.
21. Amar, M. J. A., Shamburek, R. D., Foger, B., Hoyt, R. F., Wood, D. O., Santamarina-Fojo, S., and Brewer, H. B. (1998) Adenovirus-mediated expression of LCAT in non-human primates leads to an antiatherogenic lipoprotein profile with increased HDL and decreased LDL, *Circulation Suppl. 98*, I-35.
22. Emmerich, J., Beg, O. U., Peterson, J., Previato, L., Brunzell, J. D., Brewer, H. B., Jr., and Santamarina-Fojo, S. (1992) Human lipoprotein lipase. Analysis of the catalytic triad by site-directed mutagenesis of Ser-132, Asp-156, and His-241, *J. Biol. Chem. 267*, 4161−4165.
23. Williamson, R., Lee, D., Hagaman, J., and Maeda, N. (1992) Marked reduction of high density lipoprotein cholesterol in mice genetically modified to lack apolipoprotein A-I, *Proc. Natl. Acad. Sci. U.S.A. 89*, 7134−7138.
24. Kan, H. Y., Georgopoulos, S., and Zannis, V. (2000) A hormone response element in the human apolipoprotein CIII (ApoCIII) enhancer is essential for intestinal expression of the ApoA-I and ApoCIII genes and contributes to the hepatic expression of the two linked genes in transgenic mice, *J. Biol. Chem. 275*, 30423−30431.
25. Li, X., Kan, H. Y., Lavrentiadou, S., Krieger, M., and Zannis, V. (2002) Reconstituted discoidal ApoE-phospholipid particles are ligands for the scavenger receptor BI. The amino-terminal 1−165 domain of ApoE suffices for receptor binding, *J. Biol. Chem. 277*, 21149−21157.
26. Matz, C. E., and Jonas, A. (1982) Micellar complexes of human apolipoprotein A-I with phosphatidylcholines and cholesterol prepared from cholate-lipid dispersions, *J. Biol. Chem. 257*, 4535−4540.
27. Kypreos, K. E., Van Dijk, K. W., van Der, Z. A., Havekes, L. M., and Zannis, V. I. (2001) Domains of apolipoprotein E contributing to triglyceride and cholesterol homeostasis in vivo. Carboxyl-terminal region 203−299 promotes hepatic very low-density lipoprotein-triglyceride secretion, *J. Biol. Chem. 276*, 19778−19786.
28. Bergo, M., Olivecrona, G., and Olivecrona, T. (1996) Forms of lipoprotein lipase in rat tissues: in adipose tissue the proportion of inactive lipase increases on fasting, *Biochem. J. 313* (Part 3), 893−898.
29. Yamamoto, M., Morita, S. Y., Kumon, M., Kawabe, M., Nishitsuji, K., Saito, H., Vertut-Doi, A., Nakano, M., and Handa, T. (2003) Effects of plasma apolipoproteins on lipoprotein lipase-mediated lipolysis of small and large lipid emulsions, *Biochim. Biophys. Acta 1632*, 31−39.
30. Fitzgerald, M. L., Mendez, A. J., Moore, K. J., Andersson, L. P., Panjeton, H. A., and Freeman, M. W. (2001) ATP-binding cassette transporter A1 contains an NH2-terminal signal anchor sequence that translocates the protein's first hydrophilic domain to the exoplasmic space, *J. Biol. Chem. 276*, 15137−15145.
31. Acton, S., Rigotti, A., Landschulz, K. T., Xu, S., Hobbs, H. H., and Krieger, M. (1996) Identification of scavenger receptor SR-BI as a high-density lipoprotein receptor, *Science 271*, 518−520.
32. Sege, R. D., Kozarsky, K. F., and Krieger, M. (1986) Characterization of a family of gamma-ray-induced CHO mutants demonstrates that the ldlA locus is diploid and encodes the low-density lipoprotein receptor, *Mol. Cell. Biol. 6*, 3268−3277.
33. Hill, J. S., O, K., Wang, X., Paranjape, S., Dimitrijevich, D., Lacko, A. G., and Pritchard, P. H. (1993) Expression and characterization of recombinant human lecithin:cholesterol acyltransferase, *J. Lipid Res. 34*, 1245−1251.
34. Jin, L., Lee, Y. P., and Jonas, A. (1997) Biochemical and biophysical characterization of human recombinant lecithin: cholesterol acyltransferase, *J. Lipid Res. 38*, 1085−1093.
35. Gorshkova, I. N., Liadaki, K., Gursky, O., Atkinson, D., and Zannis, V. I. (2000) Probing the lipid-free structure and stability of apolipoprotein A-I by mutation, *Biochemistry 39*, 15910−15919.
36. Gorshkova, I. N., Liu, T., Zannis, V. I., and Atkinson, D. (2002) Lipid-free structure and stability of apolipoprotein A-I: probing the central region by mutation, *Biochemistry 41*, 10529−10539.
37. Chen, Y. H., Yang, J. T., and Martinez, H. M. (1972) Determination of the secondary structures of proteins by circular dichroism and optical rotatory dispersion, *Biochemistry 11*, 4120−4131.
38. Pace, C. N., Shirley, B. A., and Thomson, J. A. (1989) in *Protein Structure* (Creighton, T. E., Ed.) pp 311−330, IRL, New York.
39. Pace, C. N., and Vanderburg, K. E. (1979) Determining globular protein stability: guanidine hydrochloride denaturation of myoglobin, *Biochemistry 18*, 288−292.
40. Pownall, H. J., Massey, J. B., Kusserow, S. K., and Gotto, A. M., Jr. (1978) Kinetics of lipid−protein interactions: interaction of apolipoprotein A-I from human plasma high-density lipoproteins with phosphatidylcholines, *Biochemistry 17*, 1183−1188.
41. Sparks, D. L., Phillips, M. C., and Lund-Katz, S. (1992) The conformation of apolipoprotein A-I in discoidal and spherical recombinant high-density lipoprotein particles. 13C NMR studies of lysine ionization behavior, *J. Biol. Chem. 267*, 25830−25838.
42. Lacowicz, J. (1999) *Principles of Fluorescence Spectroscopy*, pp 71−72, Kluwer Academic/Plenum Publishers, New York.
43. Krieger, M. (1983) Complementation of mutations in the LDL pathway of receptor-mediated endocytosis by cocultivation of LDL receptor-defective hamster cell mutants, *Cell 33*, 413−422.
44. Acton, S. L., Scherer, P. E., Lodish, H. F., and Krieger, M. (1994) Expression cloning of SR-BI, a CD36-related class B scavenger receptor, *J. Biol. Chem. 269*, 21003−21009.
45. Rigotti, A., Trigatti, B. L., Penman, M., Rayburn, H., Herz, J., and Krieger, M. (1997) A targeted mutation in the murine gene encoding the high-density lipoprotein (HDL) receptor scavenger receptor class B type I reveals its key role in HDL metabolism, *Proc. Natl. Acad. Sci. U.S.A. 94*, 12610−12615.
46. Varban, M. L., Rinninger, F., Wang, N., Fairchild-Huntress, V., Dunmore, J. H., Fang, Q., Gosselin, M. L., Dixon, K. L., Deeds, J. D., Acton, S. L., Tall, A. R., and Huszar, D. (1998) Targeted mutation reveals a central role for SR-BI in hepatic selective uptake of high-density lipoprotein cholesterol, *Proc. Natl. Acad. Sci. U.S.A. 95*, 4619−4624.
47. Zhong, S., Sharp, D. S., Grove, J. S., Bruce, C., Yano, K., Curb, J. D., and Tall, A. R. (1996) Increased coronary heart disease in Japanese-American men with mutation in the cholesteryl ester transfer protein gene despite increased HDL levels, *J. Clin. Invest 97*, 2917−2923.
48. Brousseau, M. E., O'Connor, J. J., Jr., Ordovas, J. M., Collins, D., Otvos, J. D., Massov, T., McNamara, J. R., Rubins, H. B., Robins, S. J., and Schaefer, E. J. (2002) Cholesteryl ester transfer protein TaqI B2B2 genotype is associated with higher HDL cholesterol levels and lower risk of coronary heart disease end points in men with HDL deficiency: Veterans Affairs HDL Cholesterol Intervention Trial, *Arterioscler., Thromb., Vasc. Biol. 22*, 1148−1154.

49. Busch, S. J., Barnhart, R. L., Martin, G. A., Fitzgerald, M. C., Yates, M. T., Mao, S. J., Thomas, C. E., and Jackson, R. L. (1994) Human hepatic triglyceride lipase expression reduces high-density lipoprotein and aortic cholesterol in cholesterol-fed transgenic mice, *J. Biol. Chem. 269*, 16376−16382.
50. Fan, J., Wang, J., Bensadoun, A., Lauer, S. J., Dang, Q., Mahley, R. W., and Taylor, J. M. (1994) Overexpression of hepatic lipase in transgenic rabbits leads to a marked reduction of plasma high-density lipoproteins and intermediate density lipoproteins, *Proc. Natl. Acad. Sci. U.S.A. 91*, 8724−8728.
51. Blades, B., Vega, G. L., and Grundy, S. M. (1993) Activities of lipoprotein lipase and hepatic triglyceride lipase in postheparin plasma of patients with low concentrations of HDL cholesterol, *Arterioscler. Thromb. 13*, 1227−1235.
52. McNeish, J., Aiello, R. J., Guyot, D., Turi, T., Gabel, C., Aldinger, C., Hoppe, K. L., Roach, M. L., Royer, L. J., de Wet, J., Broccardo, C., Chimini, G., and Francone, O. L. (2000) High-density lipoprotein deficiency and foam cell accumulation in mice with targeted disruption of ATP-binding cassette transporter-1, *Proc. Natl. Acad. Sci. U.S.A. 97*, 4245−4250.
53. Glomset, J. A., Norum, K. R., and Gjone, E. (1982) Familial lecithin: cholesterol acyltrasnferase deficiency, in *The Metabolic Basis of Inherited Disease* (Stanbury, J. B., Wyngaarden, J. B., Fredrickson, D. S., Goldstein, J. L., and Brown, M. S., Eds.) pp 643−654, McGraw-Hill, New York.
54. Brunzell, J. D. (1989) Familial lipoprotein lipase deficiency and other causes of the chylomicronemia syndrome, in *The Metabolic Basis of Inherited Disease* (Scriver, C. R., Beaudet, A. L., Sly, W. S., and Valle, D., Eds.) pp 1165−1180, McGraw-Hill, New York.
55. Ma, K., Cilingiroglu, M., Otvos, J. D., Ballantyne, C. M., Marian, A. J., and Chan, L. (2003) Endothelial lipase is a major genetic determinant for high-density lipoprotein concentration, structure, and metabolism, *Proc. Natl. Acad. Sci. U.S.A. 100*, 2748−2753.
56. Ishida, T., Choi, S., Kundu, R. K., Hirata, K., Rubin, E. M., Cooper, A. D., and Quertermous, T. (2003) Endothelial lipase is a major determinant of HDL level, *J. Clin. Invest. 111*, 347−355.
57. Fredrickson, D. S., Altrocchi, P. H., Avioli, L. V., Goodman, D. S., and Goodman, H. C. (1961) Tangier disease, *Ann. Intern. Med. 55*, 1016−1031.
58. Baggio, G., Manzato, E., Gabelli, C., Fellin, R., Martini, S., Enzi, G. B., Verlato, F., Baiocchi, M. R., Sprecher, D. L., Kashyap, M. L., Brewer, H. B., and Crepaldi, G. (1986) Apolipoprotein C−II deficiency syndrome. Clinical features, lipoprotein characterization, lipase activity, and correction of hypertriglyceridemia after apolipoprotein C−II administration in two affected patients, *J. Clin. Invest. 77*, 520−527.
59. Ito, Y., Azrolan, N., O'Connell, A., Walsh, A., and Breslow, J. L. (1990) Hypertriglyceridemia as a result of human apo CIII gene expression in transgenic mice, *Science 249*, 790−793.
60. de Silva, H. V., Lauer, S. J., Wang, J., Simonet, W. S., Weisgraber, K. H., Mahley, R. W., and Taylor, J. M. (1994) Overexpression of human apolipoprotein C−III in transgenic mice results in an accumulation of apolipoprotein B48 remnants that is corrected by excess apolipoprotein E, *J. Biol. Chem. 269*, 2324−2335.
61. Mensenkamp, A. R., van Luyn, M. J., van Goor, H., Bloks, V., Apostel, F., Greeve, J., Hofker, M. H., Jong, M. C., van Vlijmen, B. J., Havekes, L. M., and Kuipers, F. (2000) Hepatic lipid accumulation, altered very low density lipoprotein formation and apolipoprotein E deposition in apolipoprotein E3-Leiden transgenic mice. *J. Hepatol. 33*, 189−198.
62. Shachter, N. S., Hayek, T., Leff, T., Smith, J. D., Rosenberg, D. W., Walsh, A., Ramakrishnan, R., Goldberg, I. J., Ginsberg, H. N., and Breslow, J. L. (1994) Overexpression of apolipoprotein CII causes hypertriglyceridemia in transgenic mice, *J. Clin. Invest. 93*, 1683−1690.
63. Boisfer, E., Lambert, G., Atger, V., Tran, N. Q., Pastier, D., Benetollo, C., Trottier, J. F., Beaucamps, I., Antonucci, M., Laplaud, M., Griglio, S., Chambaz, J., and Kalopissis, A. D. (1999) Overexpression of human apolipoprotein A-II in mice induces hypertriglyceridemia due to defective very low-density lipoprotein hydrolysis, *J. Biol. Chem. 274*, 11564−11572.
64. Jong, M. C., Dahlmans, V. E., van Gorp, P. J., Van Dijk, K. W., Breuer, M. L., Hofker, M. H., and Havekes, L. M. (1996) In the absence of the low-density lipoprotein receptor, human apolipoprotein C1 overexpression in transgenic mice inhibits the hepatic uptake of very low-density lipoproteins via a receptor-associated protein-sensitive pathway, *J. Clin. Invest. 98*, 2259−2267.
65. Kypreos, K. E., Li, X., Van Dijk, K. W., Havekes, L. M., and Zannis, V. I. (2003) Molecular mechanisms of type III hyperlipoproteinemia: The contribution of the carboxy-terminal domain of apoE can account for the dyslipidemia that is associated with the E2/E2 phenotype, *Biochemistry 42*, 9841−9853.
66. Pennacchio, L. A., Olivier, M., Hubacek, J. A., Cohen, J. C., Cox, D. R., Fruchart, J. C., Krauss, R. M., and Rubin, E. M. (2001) An apolipoprotein influencing triglycerides in humans and mice revealed by comparative sequencing, *Science 294*, 169−173.
67. Fredenrich, A. (1998) Role of apolipoprotein CIII in triglyceride-rich lipoprotein metabolism, *Diabetes Metab. 24*, 490−495.
68. Havel, R. J., Kotite, L., Vigne, J. L., Kane, J. P., Tun, P., Phillips, N., and Chen, G. C. (1980) Radioimmunoassay of human arginine-rich apolipoprotein, apoprotein E. Concentration in blood plasma and lipoproteins as affected by apoprotein E-3 deficiency. *J. Clin. Invest. 66*, 1351−1362.
69. Gursky, O., and Atkinson, D. (1996) Thermal unfolding of human high-density apolipoprotein A-1: implications for a lipid-free molten globular state, *Proc. Natl. Acad. Sci. U.S.A. 93*, 2991−2995.
70. Rogers, D. P., Roberts, L. M., Lebowitz, J., Engler, J. A., and Brouillette, C. G. (1998) Structural analysis of apolipoprotein A-I: effects of amino- and carboxy-terminal deletions on the lipid-free structure, *Biochemistry 37*, 945−955.
71. Haghpassand, M., Bourassa, P. A., Francone, O. L., and Aiello, R. J. (2001) Monocyte/macrophage expression of ABCA1 has minimal contribution to plasma HDL levels, *J. Clin. Invest. 108*, 1315−1320.
72. Forte, T. M., Goth-Goldstein, R., Nordhausen, R. W., and McCall, M. R. (1993) Apolipoprotein A-I-cell membrane interaction: extracellular assembly of heterogeneous nascent HDL particles, *J. Lipid Res. 34*, 317−324.
73. Forte, T. M., Bielicki, J. K., Goth-Goldstein, R., Selmek, J., and McCall, M. R. (1995) Recruitment of cell phospholipids and cholesterol by apolipoproteins A-II and A-I: formation of nascent apolipoprotein-specific HDL that differ in size, phospholipid composition, and reactivity with LCAT, *J. Lipid Res. 36*, 148−157.
74. Fielding, C. J., and Fielding, P. E. (1995) Molecular physiology of reverse cholesterol transport, *J. Lipid Res. 36*, 211−228.
75. Chajek, T., and Fielding, C. J. (1978) Isolation and characterization of a human serum cholesteryl ester transfer protein, *Proc. Natl. Acad. Sci. U.S.A. 75*, 3445−3449.
76. Hopkins, G. J., and Barter, P. J. (1980) Transfers of esterified cholesterol and triglyceride between high density and very low-density lipoproteins: in vitro studies of rabbits and humans, *Metabolism 29*, 546−550.
77. Salinelli, S., Lo, J. Y., Mims, M. P., Zsigmond, E., Smith, L. C., and Chan, L. (1996) Structure−function relationship of lipoprotein lipase-mediated enhancement of very low density lipoprotein binding and catabolism by the low density lipoprotein receptor. Functional importance of a properly folded surface loop covering the catalytic center, *J. Biol. Chem. 271*, 21906−21913.
78. Medh, J. D., Bowen, S. L., Fry, G. L., Ruben, S., Andracki, M., Inoue, I., Lalouel, J. M., Strickland, D. K., and Chappell, D. A. (1996) Lipoprotein lipase binds to low-density lipoprotein receptors and induces receptor-mediated catabolism of very low-density lipoproteins in vitro, *J. Biol. Chem. 271*, 17073−17080.

BI049782P